# INTERPRETATION OF RADIUS OF INVESTIGATION IN COMPOSITE RESERVOIR

**V.V. Srimannarayana, M.Shyam Sundar Mohan Kumar ,Ghatty Pavan Siddharth,**

**Sai Deepika Kalisipudi , Ch. Durga Seshu , Pulla Venkata Satyanarayana**

1.Assistant Professor, Department of Petroleum Technology, Aditya Engineering College, Surampalem, A.P.

2.Associate professor, Department of Humanities and Basic Sciences, Aditya College of Engineering, Surampalem, A.P.

3. Student, Department of Petroleum Technology, Aditya Engineering College, Surampalem, A.P.

4. Student, Department of Petroleum Technology, Aditya Engineering College, Surampalem, A.P.

5. Student, Department of Petroleum Technology, Aditya Engineering College, Surampalem, A.P.

6. Student, Department of Petroleum Technology, Aditya Engineering College, Surampalem, A.P.

## Abstract

The radius of investigation is one of the primary parameters that provide us with a fundamental understanding of a reservoir in petroleum reservoir engineering or in oil and well testing. Therefore, the investigation radius is a fundamental, useful, and significant parameter to assess the well's-controlled region. In homogeneous reservoirs, the radius of inquiry is essentially considered. In homogeneous reservoirs, the investigation radius is typically calculated using an explicit function linked to the square root of time. In this study, the issue of estimating the radius of inquiry in composite reservoirs is addressed. Commercial software Saphir is used, but it is unable to interpret the radius in multi-composite zones. Then, using the calculation method for the investigation radius in a multi-zone composite reservoir derived from the investigation radius in homogeneous reservoirs, we first assumed that each zone's properties were homogeneous.

The formula for multi-zone composite reservoirs is more complex and exhibits a nonlinear implicit function in time when compared to the homogeneous reservoir's formula. We numerically calculated the dynamical investigation radii with the passage of time for both 2-zone and 3-zone composite reservoirs using the newly developed formula of the investigation radius, given a set of reservoir parameters.

For the study radii were affected over time by model parameters like permeability, porosity, and total compressibility, we therefore plotted a number of relationship curves. The relationship graphs unmistakably display a reservoir's multi-zone characteristics. The relationship graphs of N-zone composite reservoirs may show (N-1) inflection points. An inflection point is a location where a pressure wave responds to the boundary between two nearby zones. Finally, to determine the investigation radius, we used actual reservoir parameters from an

example well in a 2-zone composite reservoir. In conclusion, it has been demonstrated in this study that the newly derived formulas are a convenient and useful new tool for calculating the investigation radii in composite reservoir

# 1. Introduction

## 1.1 What is well testing

A well test in the petroleum sector is the execution of a series of organised data gathering tasks. To improve knowledge and comprehension of the hydrocarbon properties present therein as well as the features of the underground reservoir where the hydrocarbons are trapped, the acquired data is analysed.

## 1.2 Relation between well test and radius of investigation.

The extent that transient effects have travelled into the reservoir is represented by the radius of investigation. When a disturbance, such as a shift in rate, takes place at a well, a pressure transient is produced. The pressure transient moves deeper and deeper into the pool over time.

## 1.3 Purpose of estimating radius of investigation.

The main purpose of the oil well testing is to estimate the reservoir compatibility to produce the Hydrocarbons profitably. This compatibility is evaluated by different tests, out of which the pressure tests are been of top priority from the early 1950's. The pressure tests are done by increasing or decreasing the production from the well. These tests are well known as Build up tests and Drawdown tests. Due to the oil well production there will be a pressure drop in a reservoir and there will be a distribution curve of reservoir pressure in the pressure drop area which takes a shape of funnel which is usually called a "pressure drop funnel". This pressure drop funnel helps us to have an idea about oil saturation in the reservoir.
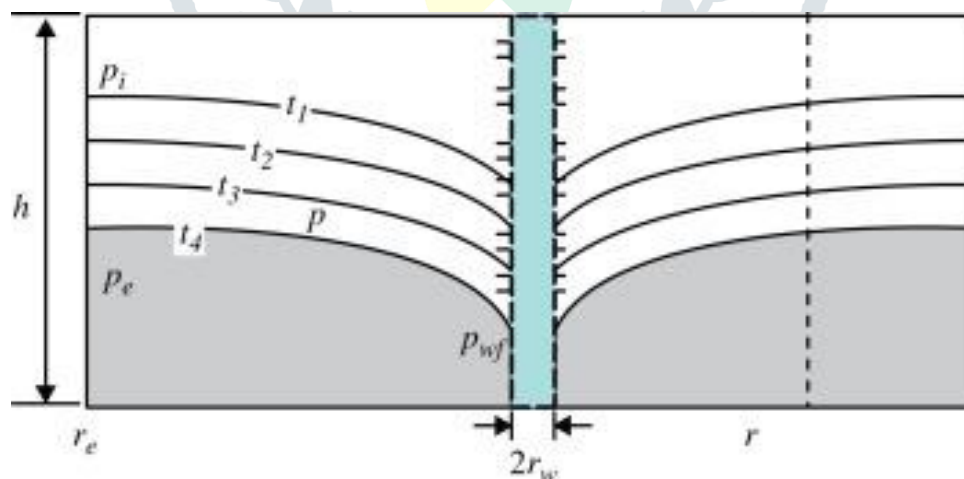


**Fig-1.1 Pressure funnel across the reservoir**

## 1.4 Theories about investigation radius in the reservoir

An investigation radius, also known as a detection radius, is the radial distance from the well's centre to the front of a pressure drop funnel or the propagating pressure reaction. The pressure drop funnel grows over time as a result of the pressure wave propagating due to well production as a result of ongoing production from the reservoir.

Therefore, it follows precisely that the inquiry radius will alter over time. The investigation radius is a product of time, to put it simply. Numerous researchers and interpreters have developed numerous theories to calculate the radius of investigations, but it wasn't until the early 1970s.

➢    "Van pollen," a pressure data interpreter, became the first to propose a calculation formula for a dimensionless investigation radius with the passage of a dimensionless amount of time for a single well production in an infinite homogeneous reservoir.

➢    Where the dimensionless time is    $r_{inv} = 2\sqrt{t_d}$.

➢    dimensionless radius is given that    $t_D = kt/[(\varphi C_t)_{m+f} \mu r_w^2]$ .

Therefore, if the parameters of the reservoir are known we can calculate the radius of investigation for the particular well the group of reservoir parameters like porosity, permeability, total compressibility of rock and fluids and fluid viscosity

According to this formula, the investigation radius is proportional to the square root of time.

Van Pollen developed this theory for homogeneous reservoirs, but because heterogeneous reservoirs can also produce hydrocarbons, there is no precise formula or dynamical model to estimate the radius of investigation in heterogeneous reservoirs. basins that combine folds, faults, fractured basins, and various sedimentary formations are known as composite reservoirs.

The data researcher is forced to dig deeper because a fault can lead to an incorrect pressure surge, which can lead to the assumption that the reservoir is empty, and fractured reservoirs can result in secondary porosities and secondary permeability. To make the well derivability accurate, pressure transients are included with the radius of inquiry to make the well produce effectively. Faults cause the pressure to escape from the micro fractures, making the data inconclusive. As a result, an accurate radius of investigation is necessary for high-quality output.

## 2. Literature review

The conventional study of composite reservoirs cannot currently be performed using the results of previous studies. To determine the radius in the heterogeneous reservoir, no straight empirical formulas are provided. Numerous people have shared their thoughts on how to simply interpret the radius of inquiry in a homogeneous reservoir. According to **Dejam** and **Hassanzadeh (2018)a and (2018)b**, if a reservoir has a closed boundary, the investigation radius ceases growing over time and equals the radius of the boundary when the pressure wave reaches it is considered as ($r_e$).

In this case, the inquiry radius for a constrained reservoir is referred to as a radius of drainage. So this is the most recent approximation, and according to these two personalities, it works well in the case of a homogeneous reservoir, especially if it has a closed boundary and is radial in characteristics. However, we frequently encounter situations where the reservoir is infinitely acting. So, this approximation does hold only for the reservoirs which are having closed boundaries. The production phase is only taken into account from the middle region of the well

test data, and it is the transient zone that provides the precise quantity of the original oil in place (OOIP). Finally, the fluid's transient flow regime in closed reservoirs at the outer boundary would be a pseudo-steady state regime.

The majority of production wells in a reservoir may actually come into contact with the drainage zones of nearby wells, causing the production wells to ultimately adopt a pseudo-steady state pressure distribution. Finally, a pseudo-steady state regime would be the fluid's transient flow regime in closed reservoirs at the outer border. The drainage zones of nearby wells may actually come into contact with the majority of production wells in a reservoir, leading the production wells to eventually assume a pseudo-steady state pressure distribution. As a result, the production well's investigation radius in infinite reservoirs must cease growing. The study radius in infinite reservoirs is also known as a "radius of drainage" in situations where the flow enters the phase of a pseudo-steady state.

The typical definition of the radius of drainage in infinite reservoirs is the radius at which the pressure shift or pressure change or flow rate was a specific percentage of that at a wellbore (for example, 0.9%) (Johnson, 1988). So, the pressure change must be imminent with respect to the wellbore to notice the change in the wellbore to get the data to be interpreted.

Numerous researchers have used various criteria to determine the drainage radius. (**Hossain et** al., 2007; **Kuchuk,** 2009). The drainage radius can be easily determined using the investigation radius method if the Time of a pseudo-steady state (tpss) is known. The duration to pseudo steady-state, or $t_{pss}$, is the name given to this period. A pressure drop, $p_t$, that is uniform and equal throughout the drainage volume from one period to the next characterises a flow regime known as pseudo steady-state. The time of the pseudo-steady state time can be calculated by using the reservoir parameters.

If the boundary effect can be graphically perceived from the well test curves, the technique of well test analysis can be used to determine the time of pseudo-steady state. (**Ishteiwy and van Poollen,** 1969; **Kazemi**, 1970).

The time of a pressure drawdown test or pressure build-up test can be used to determine the investigation radius if there is no boundary effect observed from well test curves and the curves only represent the radial Flow state in an infinite acting reservoir. (**Nie et al.,** 2018a). The pressure build up test time should we recorded and the production period and the well shut in period both should be taken into account.

The build-up test and draw down test are not only methods to find the radius of investigation in the reservoir of the infinite reservoirs, By using additional techniques in reservoir engineering, the radius of the Drainage can also be calculated. **Kutasov and Hejri (1984)** used the material balance condition to calculate the radius of outflow based on the dynamical data of well production. The dynamic data is the data, also known as transactional data, is information that is regularly updated, i.e., it changes over time as new information becomes accessible. Since the time scale of the data affects how it is processed and stored, the idea is crucial to data administration.

Numerical simulation was used by **Datta-Gupta et al. (2011)** as a substitute technique to simulate the dynamical radius of investigation over time. In summary, the investigation radius of well experiments in homogeneous reservoirs can be determined using the Formula [Formula]. What is numerical simulation? A computer calculation

carried out in accordance with a script that applies a mathematical model for a physical system is known as a numerical simulation. Most nonlinear systems have mathematical models that are too intricate for analytical solutions, necessitating the use of numerical simulations to investigate their behaviour.

Additionally, researchers have observed an issue with composite reservoirs where the initial investigation is conducted within the confines of a single well close to a sealing. Daungkaew and colleagues investigated the fault in a uniform reservoir. (2000).

In homogeneous reservoirs, the inquiry radius was defined as the reservoir made entirely of the same rock or reservoir, but what if there was a geological structure that caused disruptions in the well data? In two flow stages, a sealing fault should then be calculated independently. The formula should be used to determine the investigation radius before the pressure wave brought on by a shift in well flow rate moves to a fault.

The formula $r_{inv} = 1.623\ t_D$ can be used to determine the inquiry radius after the pressure wave has reached the fault.

Where g is a function of the relative storage capacity of the fracture system ($\omega$), an inter-porosity flow coefficient ($\lambda$), and dimensionless time, and the definition of dimensionless time is based on the overall storage capacity of the matrix and fracture systems [Equation]. In order to determine the investigation radius in naturally fractured reservoirs, Aguilera (2006) used actual well test data. So far, in the Related literature available, except for the type of homogeneous reservoirs and the type of dual porosity reservoirs, no other types of more Complex reservoirs are considered in the research of the investigation Radius.

## 3. Difference between Homogeneous reservoirs and Composite model

### 3.1 What is a Homogeneous reservoir?

Reservoir heterogeneity describes the unequal changes in the internal composition and spatial distribution of oil and gas reservoirs brought on by the effect of tectonic, diagenesis, and sedimentary processes during creation. Reservoir heterogeneity is the name for these alterations.

To obtain the oil well data and make it easier to study the factors in the homogeneous reservoir, the homogeneous reservoir characteristics should be thoroughly investigated. Analysing well test results is crucial for assessing oil and gas reserves. It uses the knowledge about the stratigraphic parameters to invert the downhole pressure as detected by pressure sensors. For instance, epidermis coefficient and wellbore storage coefficient can be obtained. Additionally, inferences can be made regarding formation characteristics, reservoir reserves, and oil output capability. We need to create a variety of stratigraphic models to establish the connection between measured pressure and stratigraphic parameters, and the homogeneous reservoir model is one typical model. The entire well test analysis procedure is shown in below.
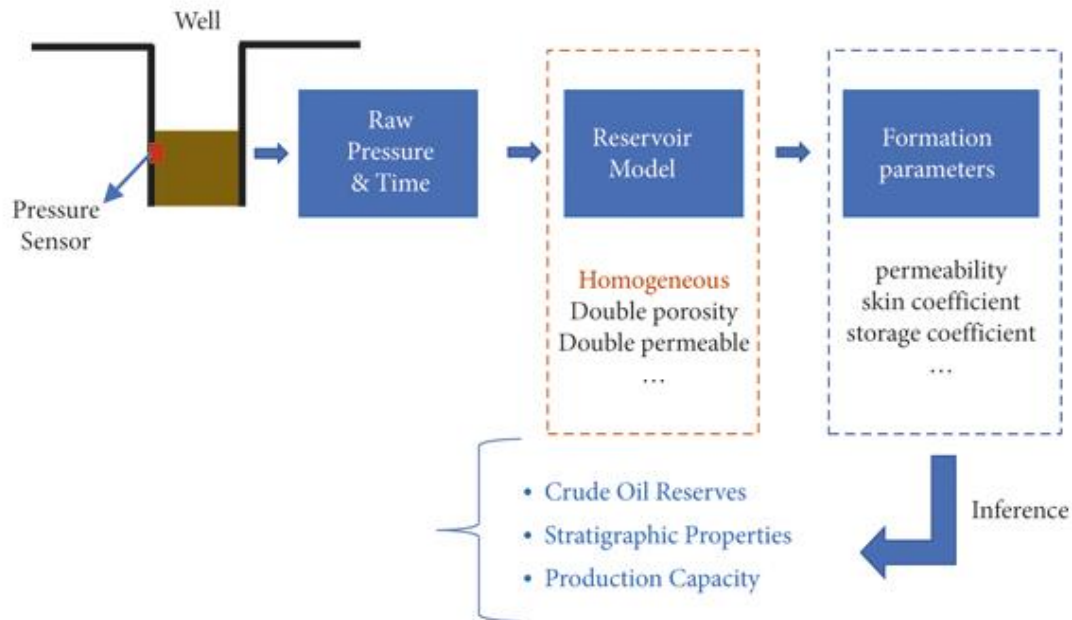
**Fig-3.1 Homogeneous model and the properties of crude**

## 3.2 Theory of Composite reservoirs

Reservoirs comprised of two overlapping zones with various hydraulic diffusivities are called composite reservoirs. What is hydraulic diffusivity, and how do composite reservoirs relate to it?

**Hydraulic conductivity**, in theory, is a measurement of the ease with which water may permeate soil or rock: high values signify permeable material, and low values signify less permeable material.

This makes a discontinuity which separates the inner and outer zones of this type of reservoir, which have uniform reservoir and fluid parameters. Reservoirs with a fluid bank, a burning front, reduced permeability around the wellbore from drilling fluid invasion, and reservoirs with increased permeability from acidizing or, roughly speaking, fracturing are examples of composite systems.

The composite reservoir alters the well's characteristics and alters the fluid's characteristics. Studies in composite reservoirs are highly challenging because of changing fluid parameters such as porosity, permeability, and viscosity.
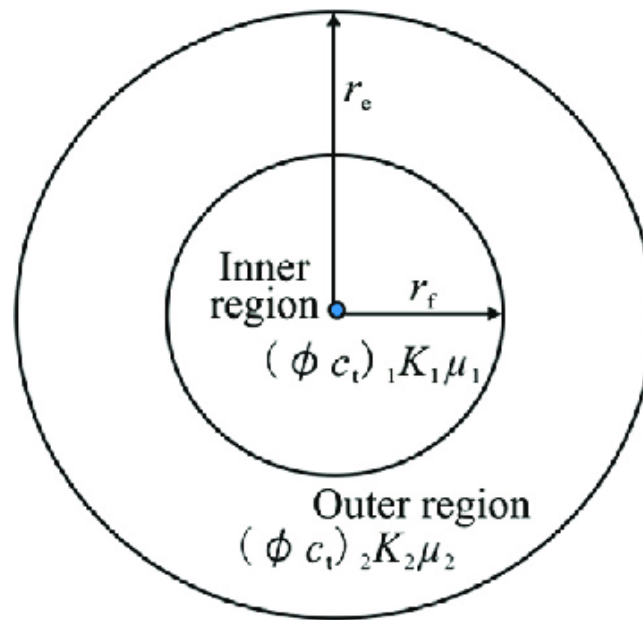
**Fig-3.2 Model of composite reservoir.**

## 4. Evaluation of Radius of investigations and its significance.

### 4.1 Testing wells using the experimental radius

Oil and gas exploration as well as other uses in the oil sector frequently face the difficulty of calculating reserves from pressure transient well test data. As a result, choosing the radius of study for a pressure transient test becomes crucial. The term transitory drainage radius is another name for it. Radius of investigation is still an ill-defined notion, despite being often employed in pressure transient testing, and there is no agreed-upon definition in the literature of petroleum.

For instance, the maximum radius in a formation when pressure has been altered during a transient well test is computed. When we apply an instantaneous source during which pressure may diffuse to a great distance, this definition is not entirely accurate.

The pressure distributions in a 1D radial-cylindrical homogenous reservoir created by a fully completed vertical well, in which the flow regime is primarily radial after the wellbore storage effect and before the effect of any outer boundary, are therefore examined first to understand the radius of investigation. Keep in mind that this might not apply to wells in heterogeneous and nonhomogeneous formations and reservoirs.

Nevertheless, knowing the fundamental radial flow regime is important to interpreting pressure transient testing and its radius of investigation i.e., how much reservoir volume is investigated for a given duration of a transient test? Running DST or production tests for exploration wells is one of the primary goals. Another is to explore the reservoir volume. Consequently, how much pressure can spread radius of investigation. So, radius of investigation is very important, and many parameters should be considered.

## 4.2 Derivation of radius of investigation in the well

"The radius of investigation concept is one of the most important concepts in pressure transient analysis. We will go through a bit of theory, define the radius of investigation, and see how we can derive it from well test analysis".

Assume that a finished vertical well, enclosed above and below by impermeable planes, is producing at a constant rate of q during t in an infinite homogeneous, isotropic reservoir with constant properties. When production begins, the reservoir is in an equilibrium condition with a constant pressure equal to Pi.

Given these circumstances, the diffusivity equation's answer is as follows:

$$Pi - p(r, \Delta t) = -\frac{q\beta\mu}{4\pi k h} Ei(-\frac{r^2}{4\eta\Delta t})$$

With the diffusivity coefficient:

$$\eta = \frac{k}{\phi \mu c_t}$$

and the exponential integral function:

$$Ei(-x) = -\int_{x}^{+\infty} \frac{e^{-u}}{u} du$$

Hence,

$$p(r, \Delta t) = P_i - \frac{q\mu B}{4\pi k h} \int_{\frac{r^2}{4\eta\Delta t}}^{\infty} \frac{e^{-u}}{u} du$$

Fortunately,

$$Ei(-x) = -\int_{x}^{+\infty} \frac{e^{-u}}{u} du \approx \ln(1.78x) \qquad for \quad small \quad values \quad of \quad x > 0$$

As a result, the solution of the diffusivity equation could be simplified as;

$$Pi - p(r, \Delta t) = -\frac{q\beta\mu}{4\pi k h} \ln(1.78 \frac{r^2}{4\eta\Delta t})$$

At the wellbore ($r = r_w$), we have.

$$Pi - p(r_w, \Delta t) = -\frac{q\beta\mu}{4\pi k h} \ln(1.78 \frac{r_w^2}{4\eta\Delta t}) = \frac{q\beta\mu}{4\pi k h} [\ln \Delta t + \ln \frac{\eta}{r_w^2} + 0.809]$$

This response defines the radial flow regime, which is the fundamental flow regime in well testing. In the bedding plane, the flow will follow the cylindrical route shown below:
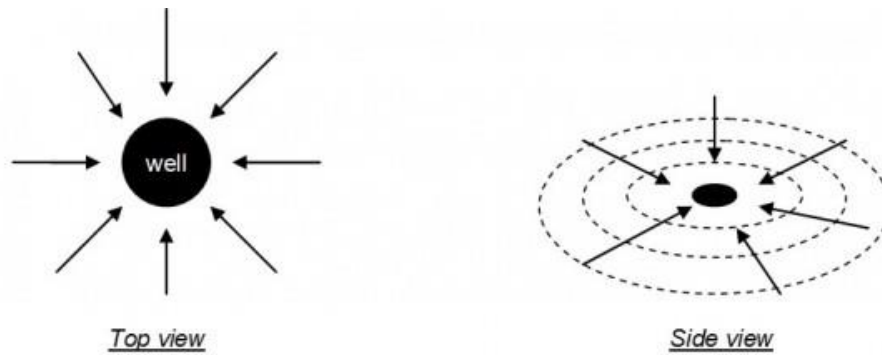
Fig-4.1 Radial view and Side view

When the output from the reservoir is established, the flowlines converge with a radial geometry in the direction of the well.

Due to output, the pressure inside the reservoir drops around the well, resulting in the following pressure change:

$$Pi - p(r, \Delta t) = \frac{q\mu B}{4\pi kh} \int_{\frac{r^2}{4\eta\Delta t}}^{\infty} \frac{1}{u} e^{-u} \, du$$

As the radius r (distance from the well) rises, the pressure change, P, also decrease with time. The transient impact is thus explained. It's important to note that the pressure disruption and well rate q are inversely related.
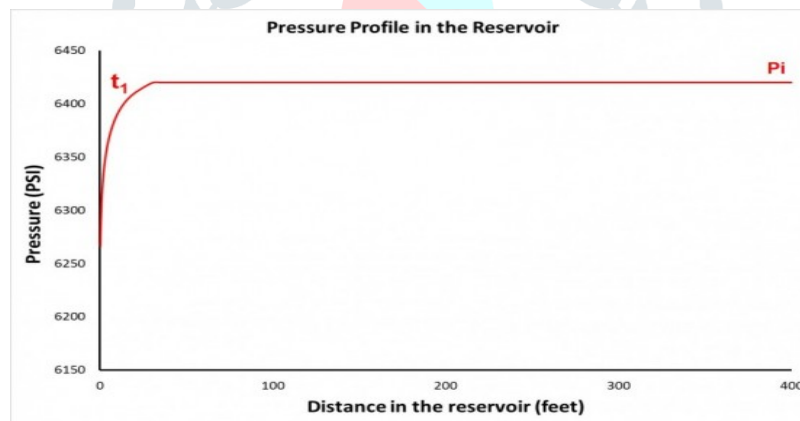


Fig- 4.2 pressure profile in the reservoir versus the radius r, at an instant t, which is created by the well producing at a constant rate q.

The minimum pressure is at the wellbore with p ($r_w$, $\Delta t$). Pressure increases with the distance from the well and tends towards the initial reservoir pressure Pi further away from the well.
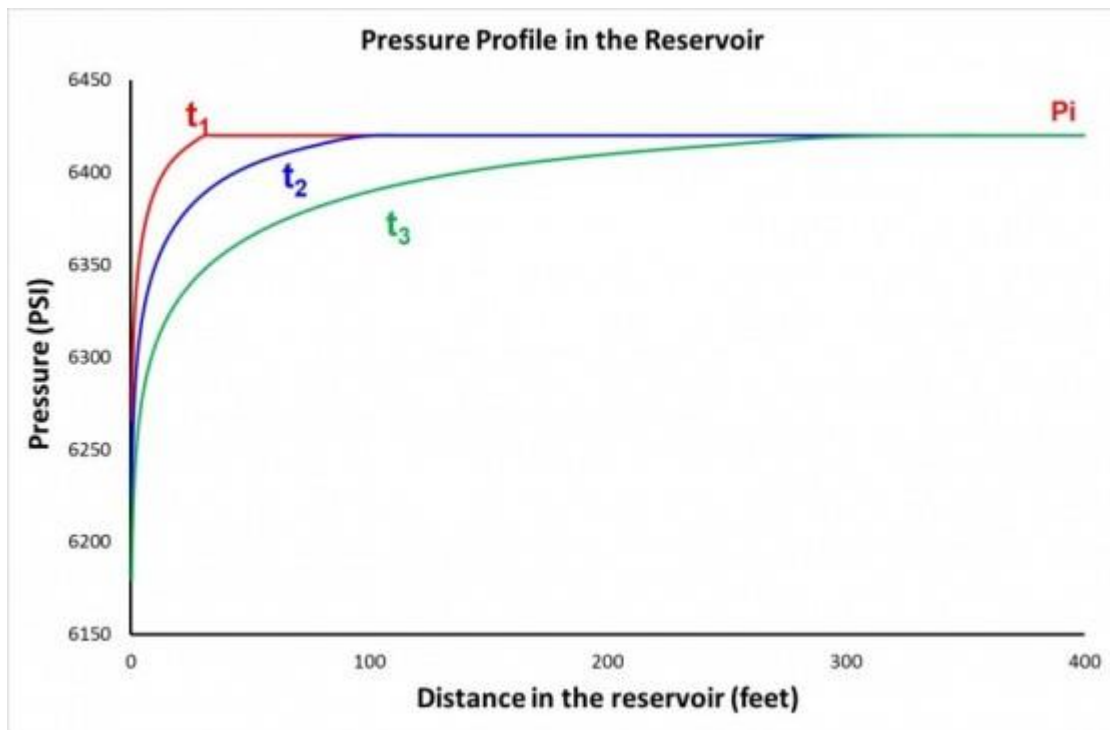
Fig-4.3 Evolution of the pressure profile as the production time increases.

$$p(R_1, \Delta t_1) = Pi - \frac{q\mu B}{4\pi kh} \int_{\frac{R_1^2}{4\eta\Delta t_1}}^{\infty} \frac{1}{u} e^{-u} \, du$$

At a time $\Delta t_2$, the pressure at the point $R_1$ and time $\Delta t_1$ will move to a distance $R_2$ in the reservoir:

$$p(R_2, \Delta t_2) = Pi - \frac{q\mu B}{4\pi kh} \int_{\frac{R_2^2}{4\eta\Delta t_2}}^{\infty} \frac{1}{u} e^{-u} \, du = p(R_1, \Delta t_1) = Pi - \frac{q\mu B}{4\pi kh} \int_{\frac{R_1^2}{4\eta\Delta t_1}}^{\infty} \frac{1}{u} e^{-u} \, du$$

:

So, we have,

$$\frac{R_2^2}{4\eta\Delta t_2} = \frac{R_1^2}{4\eta\Delta t_1}$$

As a result, the pressure that was in the reservoir at the point $R_1$ and time $\Delta t_1$ will move by the time $\Delta t_2$ to:

$$R_2 = R_1 \sqrt{\frac{\Delta t_2}{\Delta t_1}}$$

On a log scale, the pressure profile is shifted by 0.5 log($\Delta t_2$)-0.5 log($\Delta t_1$), as shown below.
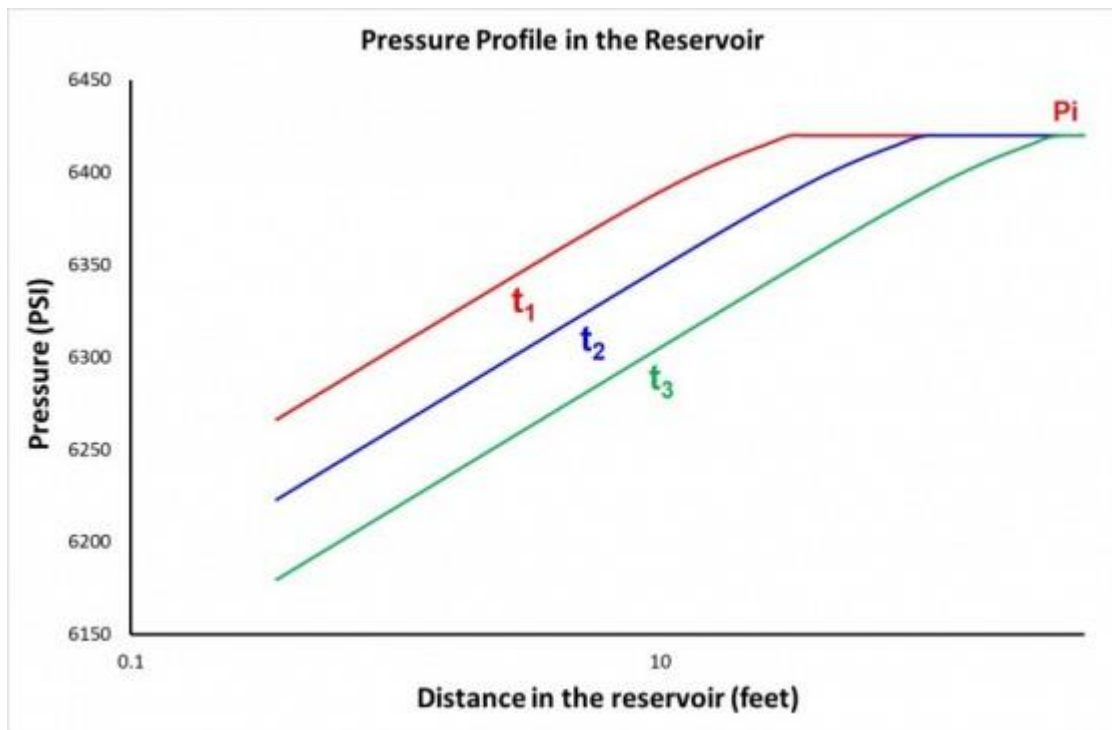
Fig-4.4 pressure profile is shifted by 0.5 log($\Delta t_2$)-0.5 log($\Delta t_1$).

As it can be observed on the figure above, a larger part of the reservoir is affected by this pressure disturbance as the production time increases. The transient response evolves away from the well.

The radius from the well to the affected reservoir region is called the radius of investigation Ri. As production time      increases,      the      radius      of      investigation      also      increases.
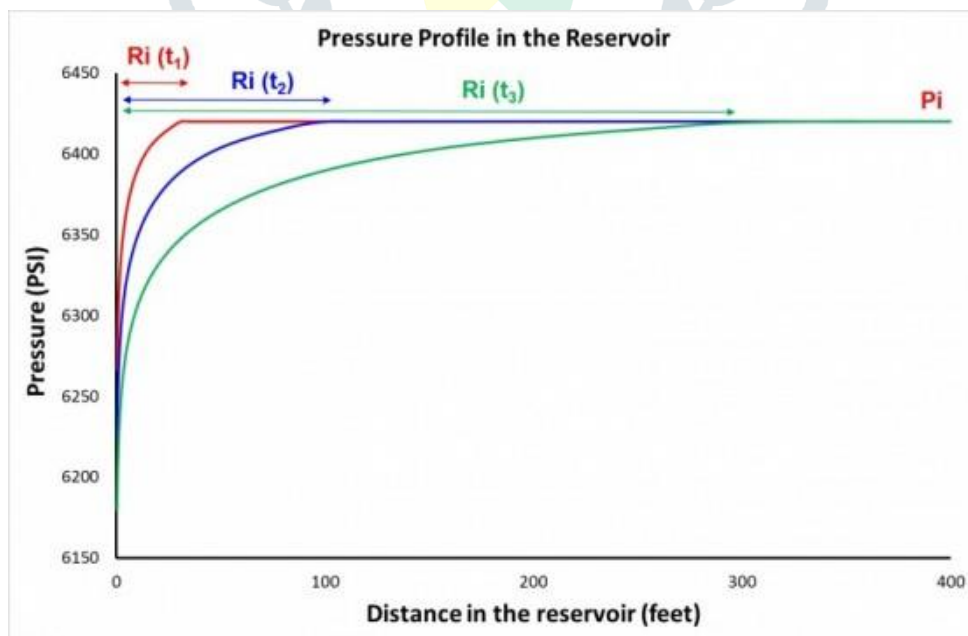


Fig-4.5 The transient response evolves away from the well.

Definition of the Radius of Investigation $R_i$

Let's first use a very simple definition of the radius of investigation at the time $\Delta t$ as $p\, R_i,\Delta t)= P_i$. At this stage, a more complex value of $R_i$ can be used.

$$Pi - p(Ri, \Delta t) = 0 = -\frac{q\beta\mu}{4\pi kh}\ln(1.78\frac{R_i^2}{4\eta\Delta t})$$

So, we have:

$$\ln(1.78\frac{Ri^2}{4\eta\Delta t}) = 0$$

And

$$1.78\frac{Ri^2}{4\eta\Delta t} = 1$$

In this case, the radius of investigation is defined as:

$$Ri = \sqrt{\frac{4\eta\Delta t}{1.78}} \approx 1.5\sqrt{\eta\Delta t}$$

Here we used a simplistic approach to define the radius of investigation. In addition, we used the log approximation of the Ei function, but this is only valid for small values of $r^2/(4\eta\Delta t)$.

When using the exponential integral function, the definition of $\Delta P= 0$ will not result in a finite $R_i$ value and therefore will not work.

We could define the radius of investigation as the point where the pressure variation is the fastest.

The pressure variation is defined as the derivative of pressure with respect to time:

$$dp(r, \Delta t)/ d\Delta t = d / d\Delta t(-\frac{q\mu B}{4\pi\, kh}\int_{\frac{r^2}{4\eta\Delta t}}^{\infty}\frac{1}{u}e^{-u}\,du) = \frac{q\mu B}{4\pi\, kh}\frac{e^{-\frac{r^2}{4\eta\Delta t}}}{\Delta t}$$

(dp/dt=dp/du.du/dt)

The maximum of the pressure variation is defined as:

$$d^2 p(r, \Delta t)/ d\Delta t^2 = \frac{q\mu B}{4\pi\, kh}\frac{e^{-\frac{r^2}{4\eta\Delta t}}}{\Delta t^2}(\frac{r^2}{4\eta\Delta t}-1) = 0$$

Hence:

$$\frac{Ri^2}{4\eta\Delta t} = 1$$

In this case, the radius of investigation is defined as:

$$Ri = \sqrt{4\eta\Delta t}$$

This results in the petroleum units:

$$Ri = \sqrt{0.0002637 \times 4\eta\Delta t} = 0.0324\sqrt{\frac{k\Delta t}{\phi\mu c_t}}$$

(Muskat, Van Poolen, Matthews & Russell, Lee, Streltsova, Bourdarot)

The radius of inquiry in oilfield units is defined in more detail below by Earlougher:

$$R_i = 0.029\sqrt{\frac{k\Delta t}{\phi\mu c_t}}$$

**More definitions of the radius of investigation are available in SPE 120515.**

The radius of inquiry grows over time by the square root of t for all these definitions. In the subsequent article, we present our third golden rule: Standard Well Test Derivative.

Additionally, we can see that the radius of inquiry is independent of rate q. The pace, however, will have an impact on the pressure signal's amplitude.

We have seen so far that the theory can be used for a constant-rate production era with a vertical well in an infinitely large homogeneous reservoir. In this instance, the flow is circular and radial towards the well, adhering to the well flow rule.

## 5. Aim of Saphir software in interpreting radius of investigation.

Even though the investigation radius is a crucial topic in well test analysis, we were unable to locate a publication on the subject in the last few years. In the area of well test analysis, recent studies have primarily concentrated on theoretical models and other application issues.

Several well test models, including fractured vertical well models, horizontal well models, and multiple fractured horizontal well models, were researched from the perspective of theory models. In terms of well test applications, new testing methods have been developed and demonstrated, and parameters like permeability and hydraulic conductivity have been determined using new methods of analysis.

However, given that we continue to run into an application issue with well test interpretations for a testing well in a composite reservoir, research on the investigation radius shouldn't be halted. In practice, a hybrid reservoir might include several locations with various reservoir characteristics.  To simulate fluid flow in this form of reservoir, a conceptual model for a multi-zone composite reservoir is typically used. **(Ambastha and Ramey, 1992; Jordan and Mattar, 2002)**.

In a multi-zone composite reservoir, however, there are currently no algorithms that can be used to determine the investigation radius of a single well. As a consequence, when selecting a model for a multi-zone composite reservoir to carry out well test interpretations, commercial software for well-test analysis (such as the well-known

"**Saphir**" created by the French company "**Kappa"**) is unable to accept a parameter value for the investigation radius.



Fig-5.1 Application problem that investigation radii in multi-zone composite reservoirs cannot be Fig gained through well test interpretations.

**5.1 Ineffectiveness of Saphir software in evaluation of radius of investigation**

This article's goal is to create a method for accurately calculating the investigation radius in multi-zone composite reservoirs. We obtain the formula for the investigation radius in 2-zone, 3-zone, and N-zone composite reservoirs, respectively, using the mass conservation principle and a conceptual model for a multi-zone composite reservoir.

We graphically display the dynamical properties of the inquiry radius over time and how key reservoir parameters like permeability and porosity affect the investigation radius. We also demonstrate how the recently discovered formula can be used to accurately determine the investigation radius in the interpretation of composite reservoir well tests.

This paper is the first research on investigation radii in multi-zone composite reservoirs because earlier studies in the literature did not address these issues. In order to conveniently acquire the values of investigation radii in well test interpretations, the formulas for investigation radii in an N-zone composite reservoir will first be derived. The suggested model in this work has some drawbacks compared to the earlier developed models in the literature, namely that faults and natural fractures are not considered.

The proposed model in this study, as well as the earlier models in the literature, also do not take into account a multiphase flow. The newly determined investigation radii formulas are still useful and applicable in well test interpretations for composite reservoirs despite these limitations in the suggested model.

The following sections will outline the work's five major steps.

➢ The application problem will be addressed first.

➢ The calculation methods for investigation radii will then be derived using a multi-zone composite reservoir model.

➢ Then will be plotted and analysed representative curves of investigation radii with time in a 2-zone composite reservoir and a 3-zone composite reservoir.

➢ After that, by using the freshly developed formulas to interpret well test results, dynamical investigation radii in a real composite reservoir will be found.

➢ Finally, a summary and conclusion will be made regarding the entire material and findings.

## 6. To interpret a Saphir issue, applying application problems in homogeneous reservoirs and composite reservoirs.

### 6.1 Case study 1- A draw-down test well in a homogeneous reservoir

The parameter of the inquiry radius can only be interpreted in the commercial well test software Saphir created by the French company Kappa when using a model for a homogeneous reservoir. As a result, we are faced with an application issue where, in the face of well test interpretations for multi-zone composite reservoirs, we are unable to determine the value of the investigation radius. By using the well test interpretations of two sample wells, we will illustrate this application problem in depth below.

In a uniform reservoir, there is a draw-down test well with the designation XY. Figure below depicts the wellbore pressure's connection to time. Porosity, thickness, and a well radius is among the fundamental reservoir characteristics that are critical for well test interpretations and are summarised in Table 6.1. Table 6.1 also displays the fluid property values, including the oil volume factor, oil viscosity, and total compressibility of rock and oil.
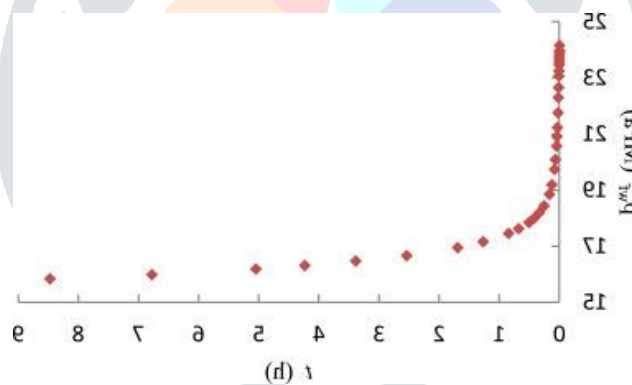


Fig-6.1. The draw-down test curve of well XY.

Table 6.1. Basic parameters of well XY for well test interpretations.

| Φ | h(m) | $r_w$ (m) | B | $\mu$ (MPa·s) | $C_t$ (MPa$^{-1}$) |
|---|------|-----------|---|---------------|---------------------|
| 0.15 | 16.15 | 0.0878 | 1.2 | 1.6 | 0.001422 |

$\varphi$ = porosity; $h$ = reservoir thickness; $r_w$ = wellbore radius; $B$ = volume factor of fluid; $\mu$ = fluid viscosity; $C_t$ = total compressibility.

For the purpose of conducting the well test analysis for well XY, we selected the Saphir model of a homogeneous reservoir with an infinite boundary. The major parameters of the modern well-test interpretation are shown in

Table 6.2, and the matched pressure and pressure derivative curves are shown in Fig 6.2. The interpretation findings indicate that well XY's investigation radius during the draw-down test period is **72.3 m**. Take note that the Saphir output interface displays the symbol as the parameter for the inquiry radius.

Table - 6.2 interpretation parameters for well XY.

| S | K(mD) | k·h (mD·m) | $p_i$ (MPa) | $r_{inv}$ (m) |
|---|---|---|---|---|
| -0.543 | 23.3 | 375 | 24.148 | 72.3 |

**S = total skin factor; k = permeability; $p_i$ = initial reservoir pressure; $r_{inv}$ = investigation radius.**



| Model Option | Standard Model |
|---|---|
| Well | Vertical |
| Reservoir | Homogeneous |
| Boundary | Infinite |
| TMatch | 119 [hr]-1 |
| PMatch | 0.732 [MPa]-1 |
| C | 0.00192 bbl/psi |
| Total Skin | -0.543 |
| k.h, total | 375 md.m |
| k, average | 23.3 md |
| Pi | 24.148 MPa |
| C | 0.00192 bbl/psi |
| Skin | -0.543 |
| Pi | 24.148 MPa |
| k.h | 375 md.m |
| k | 23.3 md |
| Rinv | 72.3 m |
| Test. Vol. | 0.250547 MMB |
| Delta P (Total Skin) | -0.74087 MPa |
| Delta P Ratio (Total Skin) | -0.0889192 Fraction |
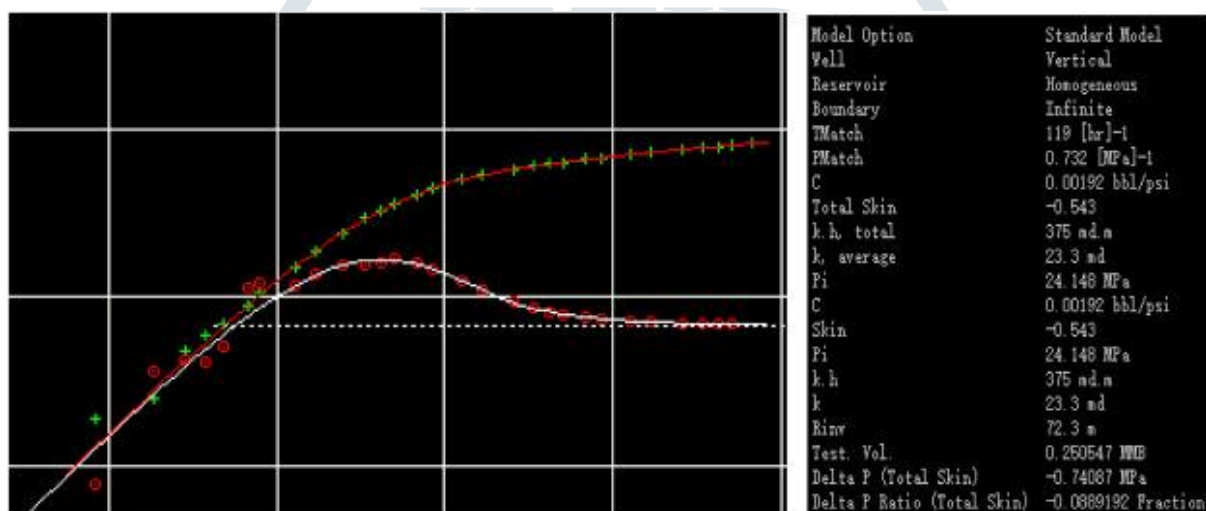
Fig-6.2 Matching curves of well test interpretation for well XY using Saphir.

## 6.2 Case study 2- A build-up test well in a 2-zone composite reservoir

In a 2-zone composite reservoir, there is a build-up test well with the designation YZ. Fig. 6.3 depicts the connection between wellbore pressure and shutting-in duration. Porosity, thickness, and a well radius is among the fundamental reservoir characteristics that are critical for well test interpretations and are summarised in Table 6.3. Table 6.3 also lists the fluid property factors, including the oil volume factor, oil viscosity, and total compressibility of rock and oil.
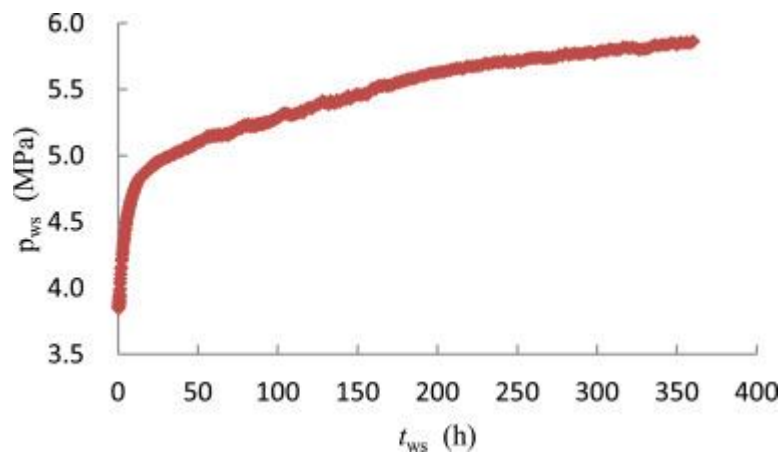
Fig-6.3. The build-up test curve of well YZ.

Table 6.3. Basic data of well YZ.

| $\Phi$ | h(m) | $r_w$ (m) | B | $\mu$ (mPa·s) | $\mu$ (mPa·s) |
|--------|------|-----------|-----|---------------|---------------|
| 0.069 | 15.39 | 0.062 | 1.069 | 57.42 | 0.001 |

φ = porosity; h = reservoir; thickness; $r_w$ = wellbore radius; B = volume factor of fluid; μ = fluid viscosity; $C_t$ = total compressibility.

To perform the well test interpretation for well YZ, we selected the Saphir model of a 2-zone composite reservoir with an infinite boundary and a changing wellbore storage model. The 2-zone composite reservoir is predicated on the notion that the reservoir is made up of two peripheral zones with various reservoir characteristics. (Olarewaju and John, 1989; Nie et al., 2011; Zhang et al., 2014).

The major parameters of the contemporary well-test interpretation are shown in Table 6.4 along with the matched pressure and pressure derivative curves. The interpretation findings indicate that we are unable to determine the well YZ's investigation radius during the build-up test period. It should be noted that the symbol "Ri" presented in Saphir's output interface denotes the inner zone's radius in the 2-zone composite reservoir rather than the investigation radius.

| Model Option | Standard Model |
|---|---|
| Well | Vertical, Changing Storage (Hegeman) |
| Reservoir | Radial composite |
| Boundary | Infinite |
| TMatch | 1.3 [hr]-1 |
| PMatch | 4.88 [MPa]-1 |
| C | 0.517 m3/MPa |
| Total Skin | -1.5 |
| k.h, total | 1730 md.m |
| k, average | 113 md |
| Pi | 7.24164 MPa |
| C | 0.517 m3/MPa |
| Ci/Cf | 7.37 |
| delta_t | 0.403 hr |
| Skin | -1.5 |
| Pi | 7.24164 MPa |
| k.h | 1730 md.m |
| k | 113 md |
| Ri | 64.2 m |
| M | 5.19 |
| D | 3.91 |
| Delta P (Total Skin) | -0.307544 MPa |
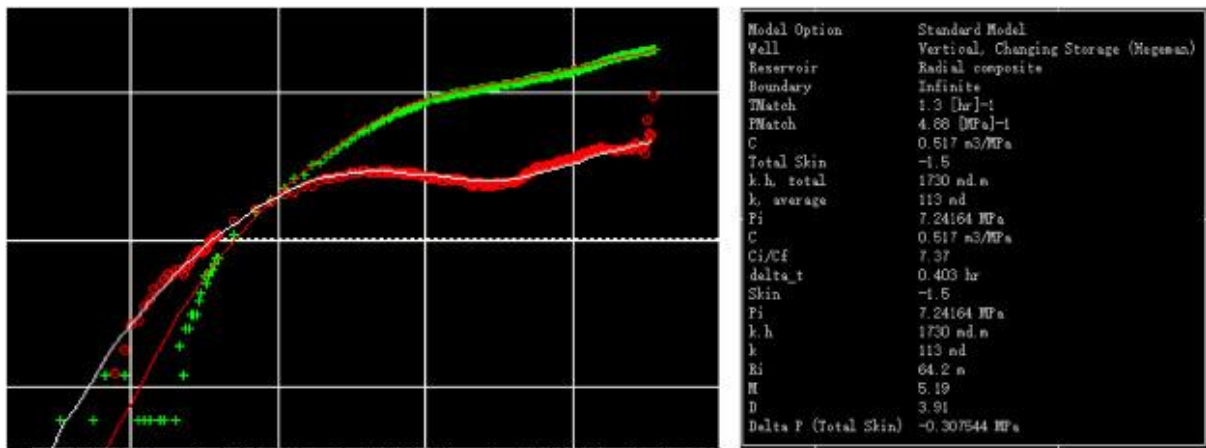
Fig.6.4. Matching curves of well test interpretation for well YZ using Saphir when choosing the composite reservoir model.

Table 6.4. Main interpretation parameters for well YZ when choosing the composite reservoir model.

| S | k(mD) | k·h (mD·m) | $p_i$ (MPa) | $r_i$ (m) | $r_{inv}$ (m) | M | D |
|---|---|---|---|---|---|---|---|
| -1.5 | 113 | 1730 | 7.24164 | 64.2 | \ | 5.19 | 3.91 |

**S = skin factor; k = permeability of inner zone; $p_i$ = initial reservoir pressure; $r_i$ = the radius of inner zone; $r_{inv}$ = investigation radius; M = the mobility ratio of inner zone to outer zone; D = the diffusivity ratio of inner zone to outer zone.**

When conducting the well test interpretation for well YZ using the Saphir homogenous reservoir model (see Fig. 6.5), we were able to determine the parameter value for the inquiry radius to be 188 m. However, as shown in Fig. 6.5 it is difficult to match the actual testing curves of well YZ, particularly the pressure derivative curve. Undoubtedly, all output parameter values are incorrect for such a well-tested explanation using an inappropriate model

.
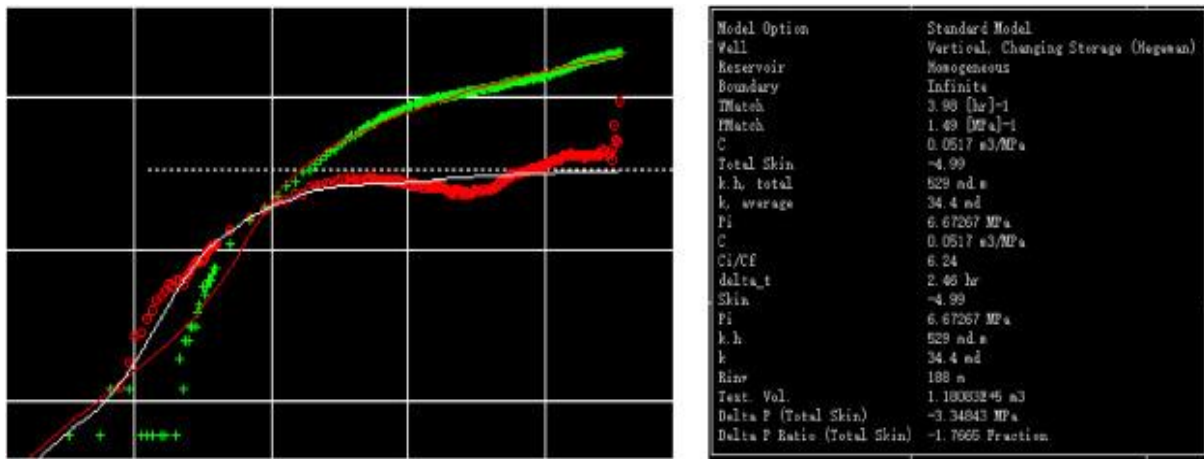
Fig. 6.5. Matching curves of well test interpretation for well XY using Saphir when choosing the homogeneous reservoir model.

We currently are unable to acquire the investigation radius in multi-zone composite reservoirs, as shown by the well test interpretations of the two field example wells discussed above. We will go into more depth about how to resolve the application problem in the following sections.

# 7. Investigation radii in multi-zone composite reservoirs

## 7.1 A multi-zone composite reservoir conceptual illustration

The investigation starts with looking below the Fig. 7.1 depicts a hypothetical model of a vertical well in a multi-zone composite reservoir. The model implies that the reservoir has N radial zones with various reservoir properties. (Olarewaju and John, 1989; Nie et al., 2011). However, it is still believed that the reservoir has homogeneous characteristics throughout each zone. The zones are labelled "1st-zone," "2nd-zone,"..., "Nth-zone," respectively, and the associated radii are marked as $r_1$, $r_2$…. and $r_N$, respectively.

The $r_N$ is typically written as re because the exterior boundary radius of the reservoir is the radius of the last zone ("Nth zone"). The subscript numbers "1," "2,"..., "N" in Fig. 14 represent the various expressions of distinct zones for various reservoir properties, including pressure (p), permeability (k), porosity (), and total compressibility of rock and fluid. (Ct). When N = 2, the model transforms into the 2-zone composite model, which consists of the interior zone (also known as the first zone), and the outer zone. (The 2nd-zone). The 3-zone composite model, which contains the inner zone (also known as the first zone), the middle zone (also known as the second zone), and the outer zone, is created when N = 3. (The 3rd-zone).

It is noteworthy that both the linear composite characteristics of a reservoir and a multiphase flow for water-producing wells are not taken into account in the model. We will deduce the calculation formula for the investigation radius below using the conceptual model of a multi-zone composite reservoir.
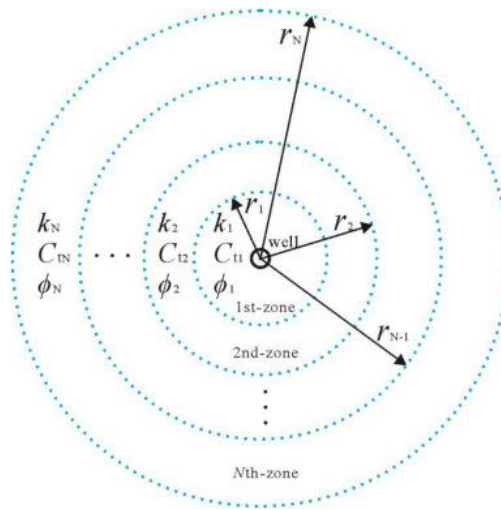
Fig.-7.1. Model scheme of a N-zone composite reservoir

## 8. Formulas of investigation radii.

### 8.1 Investigation radii in a 2-zone composite reservoir

In Appendix A, the investigation radius in a homogeneous reservoir is determined. The pressure wave will first propagate in the inner zone at a speed controlled by the diffusivity coefficient in the inner zone (1) and then propagate in the outer zone at a speed controlled by the diffusivity coefficient in the outer zone (2) given a well production at a constant sand face rate of q in a 2-zone composite reservoir.

The formula for the investigation radius, which is the same as that in a homogeneous reservoir, can be written by before the pressure wave hits the interface of the inner zone and the outer zone.

$$r_{\text{inv}}(t) = 2\sqrt{\eta_1 \cdot t} = 2\sqrt{\frac{k_1}{\varphi_1 \mu_1 C_{t1}} \cdot t} \tag{1}$$

where $r_{\text{inv}}(t)$ is the investigation radius at time t, in metres; $\eta_1$ is the first-zone's diffusivity coefficient, in $\text{m}^2/\text{s}$; t is the production time, in seconds; $k_1$ is the first-zone's permeability, in metres; $\varphi_1$ is its porosity, in %; $\mu_1$ is its fluid viscosity, in Pa; and $C_{t1}$ is its total compressibility, in $\text{Pa}^{-1}$.

The formula for the investigation radius must be newly derived once the pressure wave hits the inner-outer zone interface. After the pressure wave hits the interface, the formula for the investigation radius can be written as

$$r_{\text{inv}}^2(t) - 2r_1^2 \ln r_{\text{inv}}(t) - r_1^2 + 2r_1^2 \ln r_1 = 4\eta_2(t - t_1) \tag{2}$$

$$\eta_2 = \frac{k_2}{\varphi_2 \mu_2 C_{t2}} \tag{3}$$

where $\eta_2$ is the second zone's diffusivity coefficient (measured in $\text{m}^2/\text{s}$); $K_2$ is the second zone's permeability (measured in $\text{m}^2$); $P_2$ is the second zone's porosity (measured in percentage); $V_2$ is the second zone's fluid viscosity (measured in Pa/s); and $C_{t2}$ is the second zone's total compressibility (measured in Pa/s).

The investigation radius for a single well output in a two-zone composite reservoir can be determined using Eq. (2).

## 8.2 Investigation radii in an *N*-zone composite reservoir

The inquiry radius in an N-zone composite reservoir can be derived using the same procedure as for a 2-zone composite reservoir if N>3. This section omits the method used to derive the inquiry radius for an N-zone composite reservoir.

The calculation methods for investigation radii for numerous composite reservoirs will all be generalised in the section below.

For N = 1, an N-zone composite reservoir is just a homogenous reservoir, and the formula of the investigation radius can be expressed by,

$$r_{\text{inv}}(t) = 2\sqrt{\eta \cdot t} = 2\sqrt{\frac{k}{\varphi \mu C_t} \cdot t} \qquad (4)$$

When N = 2, an N-zone composite reservoir is simply a 2-zone composite reservoir, and the investigation radius can be calculated using the method.

$$\begin{cases} r_{\text{inv}}(t) = 2\sqrt{\eta_1 \cdot t}, (r_{\text{inv}} \le r_1, t \le t_1) \\ r_{\text{inv}}^2(t) - 2r_1^2 \ln r_{\text{inv}}(t) - r_1^2 + 2r_1^2 \ln r_1 = 4\eta_2(t - t_1), (r_{\text{inv}} > r_1, t > t_1) \\ \eta_1 = k_1/(\varphi_1 \mu_1 C_{t1}), \eta_2 = k_2/(\varphi_2 \mu_2 C_{t2}), t_1 = r_1^2/(4\eta_1) \end{cases} \qquad (5)$$

For *N* = 3, an *N*-zone composite reservoir is just a 3-zone composite reservoir, and the formula of the investigation radius can be expressed by

$$\begin{cases} r_{\text{inv}}(t) = 2\sqrt{\eta_1 \cdot t}, (r_{\text{inv}} \le r_1, t \le t_1) \\ r_{\text{inv}}^2(t) - 2r_1^2 \ln r_{\text{inv}}(t) - r_1^2 + 2r_1^2 \ln r_1 = 4\eta_2(t - t_1), \\ (r_1 < r_{\text{inv}} \le r_2, t_1 < t \le t_2) \\ r_{\text{inv}}^2(t) - 2r_2^2 \ln r_{\text{inv}}(t) - r_2^2 + 2r_2^2 \ln r_2 = 4\eta_3(t - t_2), (r_{\text{inv}} > r_2, t > t_2) \\ \eta_j = k_j/(\varphi_j \mu_j C_{tj}), t_1 = r_1^2/(4\eta_1), (j = 1,2,3) \\ t_2 = t_1 + [r_2^2 - 2r_1^2 \ln r_2 - r_1^2 + 2r_1^2 \ln r_1]/(4\eta_2) \end{cases} \qquad (6)$$

You can describe the investigation radius formula for an N-zone composite reservoir as follows:

(7)

$$
\begin{cases}
r_{\mathrm{inv}}(t) = 2\sqrt{\eta_1 \cdot t}, \, (r_{\mathrm{inv}} \le r_1, t \le t_1) \\
r_{\mathrm{inv}}^2(t) - 2r_1^2 \ln r_{\mathrm{inv}}(t) - r_1^2 + 2r_1^2 \ln r_1 = 4\eta_2(t - t_1), \\
\quad (r_1 < r_{\mathrm{inv}} \le r_2, t_1 < t \le t_2) \\
r_{\mathrm{inv}}^2(t) - 2r_2^2 \ln r_{\mathrm{inv}}(t) - r_2^2 + 2r_2^2 \ln r_2 = 4\eta_3(t - t_2), \\
\quad (r_2 < r_{\mathrm{inv}} \le r_3, t_2 < t \le t_3) \\
\qquad\qquad \vdots \\
r_{\mathrm{inv}}^2(t) - 2r_{N-2}^2 \ln r_{\mathrm{inv}}(t) - r_{N-2}^2 + 2r_{N-2}^2 \ln r_{N-2} = 4\eta_{N-1}(t - t_{N-2}), \\
\qquad\qquad\qquad (r_{N-2} < r_{\mathrm{inv}} \le r_{N-1}, t_{N-2} < t \le t_{N-1}) \\
r_{\mathrm{inv}}^2(t) - 2r_{N-1}^2 \ln r_{\mathrm{inv}}(t) - r_{N-1}^2 + 2r_{N-1}^2 \ln r_{N-1} = 4\eta_N(t - t_{N-1}), \\
\quad (r_{\mathrm{inv}} > r_{N-1}, t > t_{N-1}) \\
\eta_j = k_j / (\varphi_j \mu_j C_{tj}), \, t_1 = r_1^2 / (4\eta_1), \, (j = 1,2,3,\cdots,N) \\
t_k = t_{k-1} + \left[ r_k^2 - 2r_{k-1}^2 \ln r_k - r_{k-1}^2 + 2r_{k-1}^2 \ln r_{k-1} \right] / (4\eta_k), \, (k = 2,3,\cdots,N)
\end{cases}
$$

where $\eta_j$ is the diffusivity coefficient of the $j^{\mathrm{th}}$-zone, m²/s; $k_j$ is the $j^{\mathrm{th}}$-zone permeability, m²; $\varphi_j$ is the porosity of the $j^{\mathrm{th}}$-zone, fraction; $\mu_j$ is the fluid viscosity in the $j^{\mathrm{th}}$-zone, Pa·s; $r_j$ is the radial radius of the $j^{\mathrm{th}}$-zone, m; $t_j$ is the time when the pressure wave reaches the radial radius of the $j^{\mathrm{th}}$-zone, s; the subscripts j or k represents a zone number of a multiple composite reservoir.

Equations (5), (6), and (7), which are nonlinear transcendental equations, display a nonlinear implicit function linked to time. Iteration techniques, such as the Newton iteration approach, can be used to solve these transcendental equations.

## 9. Typical curves of investigation radii with time.

The inquiry radius is a function of production time and is governed by reservoir property parameters such as permeability, porosity, and total compressibility of rock and fluid, according to the derived formulas of investigation radii for multiple composite reservoirs. As a result, using Eq. (7), we can sketch a relationship curve of an investigation radius with time if a set of reservoir property parameters is provided. From there, we can examine the dynamical properties of this radius. Additionally, by simulating the relationship curves that are affected by a variety of reservoir property parameters, we can examine how sensitive normal curves are to various parameters.

In the sections that follow, we will compute, plot, and analyse the typical curves of investigation radii using examples of a 2-zone composite reservoir and a 3-zone composite reservoir.

### 9.1 Typical curves of investigation radius in 2-zone composite reservoir.

In this part, we use Eq. to determine the investigation radius of a 2-zone composite reservoir by using the values of the reservoir property parameters from the aforementioned well YZ. (5). Tables 6.3 and 6.4 provide the following fundamental information about various parameters: The first zone's radius ($r_1$) is 64.2 meters, its

permeability ($k_1$) is 113 metres per second, its porosity ($\varphi_1$) is 0.069 metres per second, its fluid viscosity ($\mu_1 = \mu_2$) is 57.42 metres per second, and its total compressibility ($C_{t1}$) is 0.001 MPa.

The mobility ratio of the first zone to the second zone (M) is 5.19, the diffusivity ratio of the first zone to the second zone (D) is 3.91, the permeability of the second zone ($k_2$) is 21.77 mD, the total compressibility of the second zone ($C_{t2}$) is 0.0009 MPa1, and the second zone porosity ($\varphi_2$) is 0.058. Remember that using the mobility and diffusivity rates, respectively, you can determine the 2nd-zone permeability and diffusivity. (see Table 6.4).

We specifically change the 2nd-zone permeability from 21.77mD to 31.77mD, 41.77mD to 51.77mD, and 61.77mD in order to examine the sensitivity of typical curves to this parameter. We determined a collection of constant parameter values for the following other property parameters in order to calculate the investigation radius: $k_1$ is equal to 113 mD, $\varphi_1$ is 0.069, $C_{t1}2$ is 0.058, $C_{t1}$ is 0.001 MPa$^{-1}$, $C_{t2}$ is 0.0009 MPa$^{-1}$, 1 is $\mu_2$ is 57.42 mPas, and $r_1$ is 64.2 m. The relationship curves of the inquiry radius with time for various values of the 2nd-zone permeability are shown in Fig.9.1. This figure demonstrates that the investigation radius does not grow linearly with passing time. Additionally, we can observe that the curves have an inflection point that corresponds to the pressure wave's reaction to the first zone second-zone contact.

The first-zone curve, which represents the propagation of pressure waves in the first-zone region, and the second-zone curve, which represents the propagation of pressure waves in the second-zone region, can be separated into two sections in a typical curve of the investigation radius. 36128 seconds (10.036 hours) pass during pressure wave propagation to the contact (t1). Furthermore, it is clear that the 2nd-zone permeability only affects where the 2nd-zone arcs are located. The location of the second-zone curve is higher the greater the second-zone permeability. A higher curve indicates a larger radius of inquiry for the same production time because the pressure wave propagates more quickly in a reservoir with a higher relative permeability level.
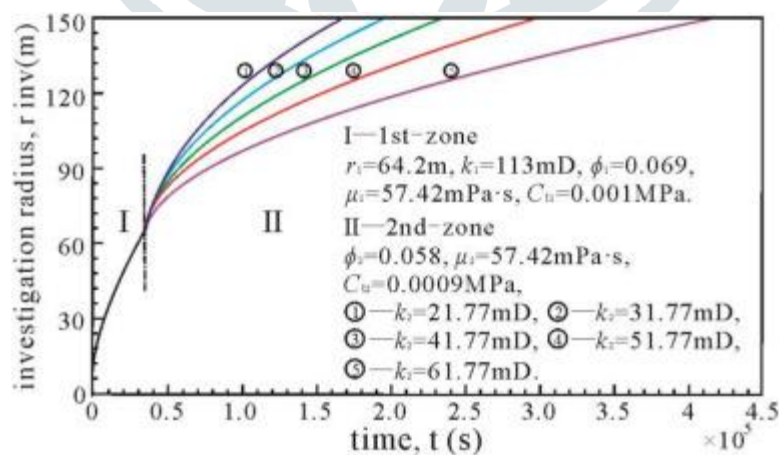


Fig-9.1. Typical curves influenced by the 2nd-zone permeability.

We specifically alter the 2nd-zone porosity from 0.058, to 0.068, to 0.078, to 0.088, and to 0.098 in order to model the typical curves affected by the 2nd-zone porosity. The following property values are used to calculate the investigation radius: $k_1$ = 113 mD, $k_2$ = 21.77 mD, $\varphi_1$ = 0.069, $C_{t1}$ = 0.001 MPa$^{-1}$, $C_{t2}$ = 0.0009 MPa$^{-1}$, $\mu_1 = \mu_2$ = 57.42 mPa-s, and $r_1$ = 64.2 m. The usual curves of the investigation radius with time under various 2nd-zone

porosity values are shown in Fig. 9.2. The position of the second-zone curves is clearly influenced by the second-zone porosity as can be seen in the figure. Diffusivity is defined as

$\eta = k/(\varphi \mu C_t)$, which implies that porosity is negatively proportional to diffusivity and that a greater porosity results in a weaker ability of the pressure wave to diffuse. For the same production period, a smaller radius of investigation results from bigger 2nd-zone porosity and lower 2nd-zone curve location.
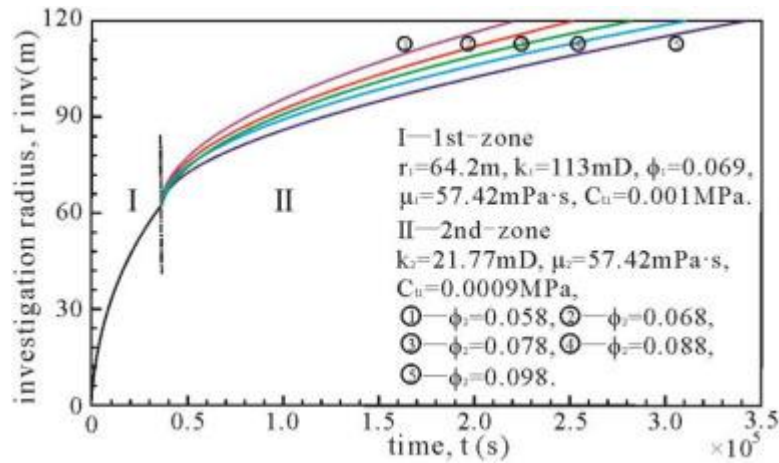


Fig-9.2. Typical curves influenced by the 2nd-zone porosity.

The typical curves of the investigation radius affected by the overall compressibility of the second-zone are shown in Fig. 17. The typical curves were simulated by using a group of fixed reservoir property parameters ($k_1 = 113$mD, $k_2 = 21.77$mD, $\varphi_1 = 0.069$, $\varphi_2 = 0.058$, $C_{t1} = 0.001$ MPa$^{-1}$, $\mu_1 = \mu_2 = 57.42$ mPa·s, $r_1 = 64.2$ m) and setting various values for the total compressibility of the 2nd-zone from 0.0009 MPa$^{-1}$, to 0.00092 MPa$^{-1}$, to 0.00094 MPa$^{-1}$, to 0.00096 MPa$^{-1}$, and to 0.00098 MPa$^{-1}$.

The relationship between diffusivity and total compressibility is inverse, as stated by the equation of diffusivity, $= k/(\varphi \mu C_t)$. As a consequence, for the same production time, a higher total compressibility of the second-zone leads to a lower location of the second-zone curve and a smaller radius of investigation, as shown in Fig. 9.3.
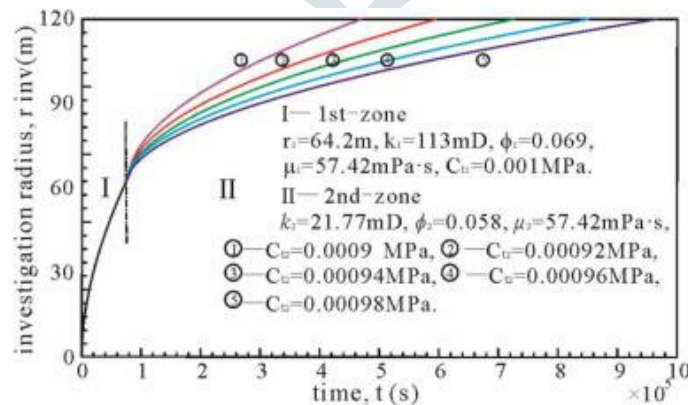


Fig-9.3 Typical curves influenced by the total 2nd-zone compressibility.

The typical curves of the investigation radius as affected by the first-zone radius are shown in Fig. 11. The typical curves were simulated by using a set of fixed reservoir property parameters ($k_1 = 113$ mD, $k_2 = 21.77$ mD, $\varphi_1 =$

0.069, $\varphi_2 = 0.047$, $C_{t1} = 0.001$ MPa$^{-1}$, $C_{t2} = 0.0009$ MPa$^{-1}$, $\mu_1 = \mu_2 = 57.42$ mPa-s) and changing the 1st-zone radius to different values between 64 m and 250 m.

The inflection points in a curve shift to the higher right as the radius of the first zone increases, as shown in Fig. 9.4. This is because the pressure wave's reaction to the interface between the first and second zones delays. As a result, the pressure wave's travel time ($t_1$) to the interface shifts from 36128 seconds (10.036 hours) to 87654 seconds (24.35 hours), 197222 seconds (54.78 hours), 350618 seconds (97.39 hours), and 547840 seconds (152.18 hours), respectively.
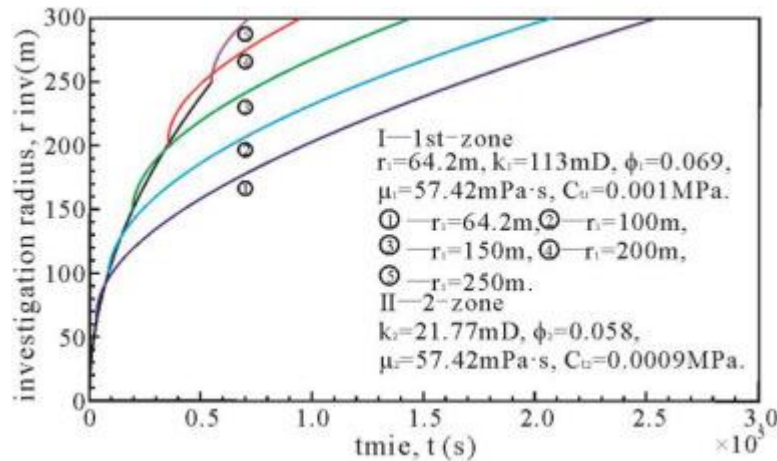


Fig-9.4. Typical curves influenced by the 1st-zone radius.

## 9.2 Investigation radius in a 3-zone composite reservoir

In this section, we set the following parameter values as the basic data to calculate the investigation radius: $k_1 = 113$mD, $k_2 = 21.77$mD, $k_3 = 10$mD, $\varphi_1 = 0.069$, $\varphi_2 = 0.058$, $\varphi_3 = 0.047$, $\mu_1 = \mu_2 = \mu_3 = 57.42$ mPa·s, $C_{t1} = 0.001$ MPa$^{-1}$, $C_{t2} = 0.0009$ MPa$^{-1}$, $C_{t3} = 0.00095$ MPa$^{-1}$, $r_1 = 64.2$ m, and $r_2 = 100$ m

We specifically change the 3rd-zone permeability from 5mD to 10mD to 15mD to 20mD to 25mD in order to examine the sensitivity of typical curves to the permeability of the third zone. Figure 9 depicts the relationship curves between the investigation radius and duration for various third-zone permeability values. This image demonstrates how the investigation radius continues to grow nonlinearly over time. There are two inflection spots in the typical curves in the third-zone composite reservoir fig (19) when compared to the typical curves in the two-zone composite reservoir (see Fig. 9.5).

The first inflection point represents the response of pressure wave to the interface between the 1st-zone and the 2nd-zone (the first interface), and the second inflection point represents the response of pressure wave to the interface between the 2nd-zone and the 3rd-zone (the second interface).

Of course, a normal curve of the investigation radius can be divided into three sections, each of which represents

the pressure wave's propagation in the first, second, and third zones. The first and second contacts' respective pressure wave propagation times are 36128 s (10.04 h) and 112721 s (36.31 h). The third-zone permeability only affects the position of the third-zone curve, as the image also shows. The radius of inquiry grows as the third-zone permeability rises, and for a given production time, the 3rd-zone curve moves higher in location.
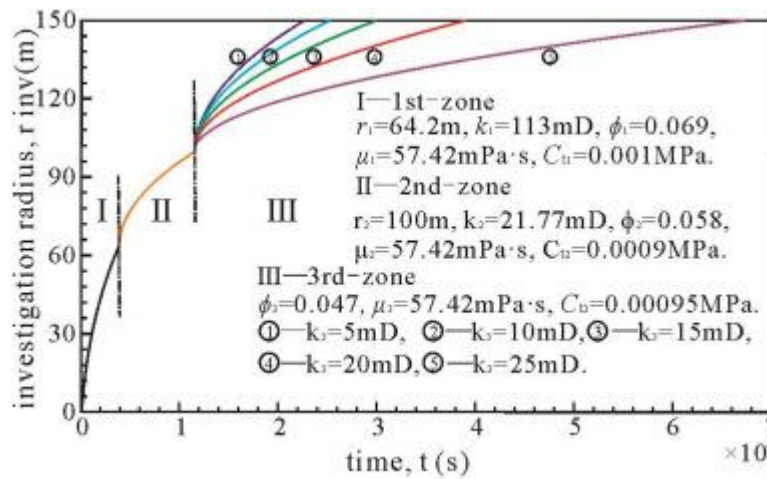


Fig-9.5. Typical curves influenced by the 3rd-zone permeability.

The typical curves in the 3-zone composite reservoirs were simulated by setting various values for the 2nd-zone radius from 120 m to 140 m, to 160 m, to 180 m, and 200 m, as shown in fig. (9.6). Apparently, the 2nd-zone radius has much influence on the typical curves of the investigation radius.

With an increase in the 2nd-zone radius, the response of pressure wave to the second interface delays, which makes the second inflection point in a curve to move towards upper right, as shown in fig. (9.6). Accordingly, the propagation time ($t_2$) of pressure wave to the second interface varies from 212439 s (59.01 h) to 347686 s (96.61 h), to 516320 s (143.4224 h), to 716960 s (199.16 h), and to 948660 s (263.52 h), respectively.
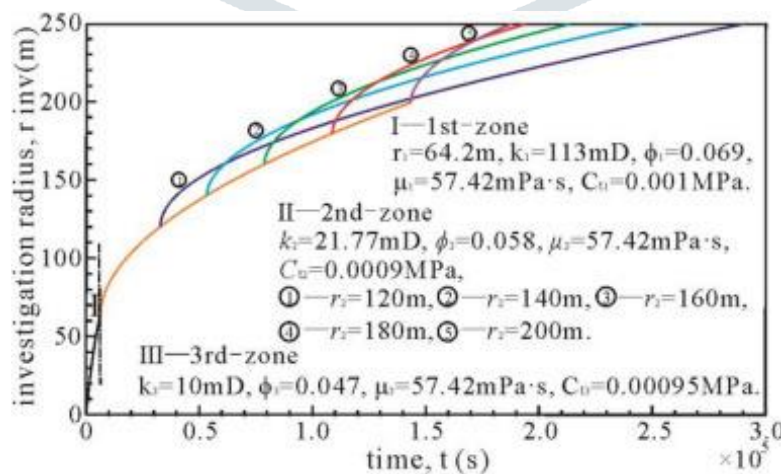


Fig-9.6. Typical curves influenced by the 2nd-zone radius.

The porosity and total compressibility of the 3-zone composite reservoir have a comparable effect on a typical curve as the 2-zone composite reservoir, so the sensitivities of typical curves to porosity and total compressibility are not examined here.

To summarize, we can plot the typical curves of the investigation radius with time in N-zone composite reservoirs using a similar technique and analyse how sensitive the typical curves are to various parameters. In a composite N-zone reservoir, the usual curves show (N-1) inflection spots. A pressure wave's reaction to the interface between two adjacent zones is represented by an inflection point. By using the (N-1) inflection points, one can split typical curves into N parts.

Each section's curve has a distinct shape because a curve shows how a pressure wave spreads in a different area with various reservoir characteristics. There is a matching composite region for each part. If the curves of the $j_{th}$-part are referred to as the $j_{th}$-zone curve, for instance, the $j_{th}$-zone curve represents the propagation of the pressure wave in the $j_{th}$-zone region (j = 1, 2,, N).

In numerous composite reservoirs, typical curves are dependent on the reservoir's characteristics. The capacity of pressure waves to diffuse in reservoirs is typically described by the diffusivity parameter. Diffusivity is defined as being inversely proportionate to porosity and total compressibility and proportional to reservoir permeability.

Diffusivity increases with increasing permeability, decreasing porosity, or decreasing overall compressibility. The speed at which the pressure pulse spreads in reservoirs is inversely proportional to the diffusivity. As a result, if the production time remains constant, the radius of inquiry grows as diffusivity rises, which elevates the location of a typical curve.

The usual curves of the investigation radius are greatly influenced by the radius of each zone as well. The corresponding inflection point in the curve shifts towards the upper right as the radius of each zone increases because the response of the pressure wave to the associated interface delays.

## 10. Real case application.

We have already shown in the second part of this article how the investigation radius cannot be determined using the build-up testing data from well YZ from a 2-zone composite reservoir by the commercial software Saphir. Using the recently discovered investigation radius method  (by looking into Eq. (5), we will determine the investigation radius of well YZ below. On the basis of the basic data and the well test interpretation results of well YZ (by looking into Table 6.3, Table 6.4), the parameters needed for the calculation of the investigation radius are prepared as follows: The radius of the 1st-zone ($r_1$) is 64.2 m, the 1st-zone permeability ($k_I$) is 113mD, the 1st-zone porosity ($\varphi_1$) is 0.069, the fluid viscosity ($\mu_1$) is 57.42 mPa·s, the total compressibility of the 1st-zone ($C_{t1}$) is 0.001 MPa$^{-1}$, and the diffusivity ratio of the 1st-zone to the 2nd-zone (D) is 3.91. First, according to the definition of diffusivity, $\eta = k/(\varphi\mu C_t)$, we calculated the 1st-zone diffusivity ($\eta_1 = 0.0285 \, \text{m}^2/\text{s}$). Then, we calculated the 2nd-zone diffusivity ($\eta_2 = 0.00729 \, \text{m}^2/\text{s}$) by use of the 1st-zone diffusivity ($\eta_1$) and the diffusivity ratio of the 1st-zone to the 2nd-zone (D). Furthermore, we ascertained the time at which pressure wave propagates to the interface ($t_1 = 36128\text{s} = 10.04 \, h$). We substitute the above parameter values into Eq. (5)

$$\begin{cases} r_{\text{inv}}(t) = 0.3376\sqrt{t}, (t \leq 36128\text{s}) \\ r_{\text{inv}}^2(t) - 8243.28 \ln r_{\text{inv}}(t) - 0.0292t + 31241.86 = 0, (t > 36128\text{s}) \end{cases} \qquad (8)$$

To determine the well X2's exploration radius, use equation (8). The relationship curve between the investigation radius and the shut-in time of the build-up well test for well YZ was plotted after the transcendental equation was solved using the Newton iteration technique, as shown in Fig10.1. Well, YZ's longest shut-in period is 360.3 hours. (1297080s). As a result, the inquiry radius of well YZ at the conclusion of the build-up well test is 226.58 m.
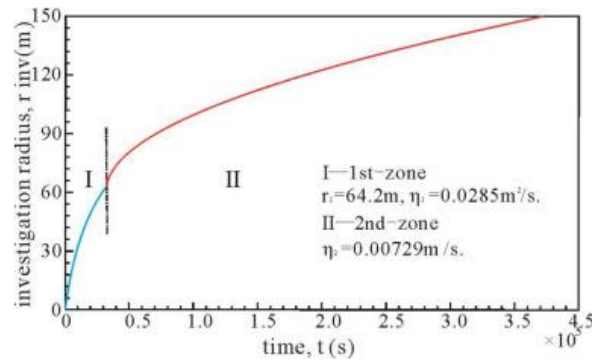


Fig-10.1. Relationship curve of investigation radius with shut-in time for well X2

## 11. Conclusion and summary.

In summary, based on the conceptual model of an N-zone composite reservoir, a series of calculation formulas of investigation radii in multiple composite reservoirs were derived and a series of typical curves of the investigation radii with time were also simulated and analysed. The newly derived formulas are convenient to gain a value of investigation radii in multi-zone composite reservoirs. The modelling analysis technique is simple to comprehend, and it can be used repeatedly for research purposes. The modelling analysis technique used in this paper effectively solves the application problem that is proposed. These are the conclusions:

➢ The recently discovered equations for the investigation radii when N-2 are nonlinear transcendental equations that can be resolved through iterative techniques.

➢ The typical curves demonstrate that the investigation radius grows nonlinearly with time and that the curve shape appears to demonstrate the multi-zone characteristics of a composite reservoir.

➢ The usual curves of an N-zone composite reservoir contain (N-1) inflection points, which signify the pressure wave's reaction to an interface between two adjacent zones.

➢ The typical curves can be divided into N parts using the (N-1) inflection points, each of which has a matching composite region and different-shaped typical curves.

➢ In numerous composite reservoirs, typical curves are dependent on the reservoir's characteristics. A typical curve is located higher when the permeability, porosity, or total compressibility are greater. Each zone's associated inflection point moves towards the upper right as its radius grows.

➢ The recently developed formulas can be used to estimate the investigation radii for multi-zone composite reservoirs, according to a successful actual case application.

## ➢ References

1. Ishteiwy, A.A., van Poollen, H.K., 1969. Radius-of-drainage equation for pressure build-up. In: SPE-2468-MS. Libyan Association of Petroleum Technologists' Annual Meeting.

2. Johnson, P.W., 1988. The relationship between radius of drainage and cumulative pro-duction. SPE Form. Eval. 3 (1), 267–270 SPE-16035-PA.

3. Jordan, C.L., Mattar, L., 2002. Comprehensive application of a composite reservoir model to pressure-transient analysis. J. Can. Pet. Technol. 41 (2), 15–23 PETSOC- 02-02-03.

4. Kamal, M.M., Morsy, S., Suleen, F., Pan, Y., Dastan, A., Stuart, M.R., Mire, E., Zakariya, Z., 2019. Determination of in-situ reservoir absolute permeability under multiphase-flow conditions using transient well testing. SPE Reserve. Eval. Eng. 22 (1), 336–350.

5. Kazemi, H., 1970. Pressure buildup in reservoir limit testing of stratified systems. J. Pet. Technol. 22 (4), 503–511 SPE-2618-PA.

6. Klammler, H., Layton, L., Nemer, B., Hatfield, K., Mohseni, A., 2017. Theoretical aspects for estimating anisotropic saturated hydraulic conductivity from in-well or direct-push probe injection tests in uniform media. Adv. Water Resource. 104, 242–254.

7. Kuchuk, F.J., 2009. Radius of investigation for reserve estimation from pressure transient well tests. In: SPE-120515-MS. SPE Middle East Oil and Gas Show and Conference, 15-18 March, Manama, Bahrain.

8. Kutasov, I.M., Hejri, S., 1984. Drainage radius of a well produced at constant bottomhole pressure in an infinite acting reservoir. In: SPE-13382-MS. Society of Petroleum Engineers.

9. Marshall, S.L., 2009. Nonlinear pressure diffusion in flow of compressible liquids through porous media. Transp. Porous Media 77 (3), 431–446.

10. Mashayekhizadeh, V., Dejam, M., Ghazanfari, M.H., 2011. The application of numerical Laplace inversion methods for type curve development in well testing: a comparative study. Pet. Sci. Technol. 29 (7), 695–707.

11. Nie, R.S., Guo, J.C., Jia, Y.L., Zhu, S.Q., Rao, Z., Zhang, C.G., 2011. New modelling of transient well test and rate decline analysis for a horizontal well in a multiple-zone reservoir. J. Geophys. Eng. 8 (3), 464–467.

12. Nie, R.S., Ou, J.J., Wang, S.R., Deng, Q., Qin, M., Jia, J.W., Wang, Y.M., 2018a. Time- tracking tests and interpretation for a horizontal well at different wellbore positions. Interpret. J. Subsurf. Charact. 6 (3), T699–T712.

13. Nie, R.S., Wang, Y.M., Kang, Y.L., Jia, Y.Lu, 2018b. Modeling the characteristics of Bingham porous-flow mechanics for a horizontal well in a heavy oil reservoir. J. Pet. Sci. Eng. 171, 71–81.

14. Olarewaju, J.S., John, W., 1989. Comprehensive application of a composite reservoir model to pressure-transient analysis. SPE Reserv. Eng. 4 (3), 325–331 SPE-16345-PA. Sabet, M.A., 1991. Well Test Analysis. Publisher: Gulf Publishing Company, Houston, Texas.

15. Sobbi, F.A., Badakhshan, A., 1996. Radius of investigation for well tests in dual porosity reservoirs. J. Can. Pet. Technol. 35 (6), 49–54 PETSOC-96-06-05.

16. van Poollen, H.K., 1964. Radius-of-drainage and stabilization-time equations. Oil Gas J. 62 (4), 138–164.

17. Wang, X.L., Fan, X.Y., He, Y.M., Nie, R.S., Huang, Q.H., 2013. A nonlinear model for fluid flow in a multiple-zone composite reservoir including the quadratic gradient term.

18.  Geophys. Eng. 10 (4), 1–11. Wang, Y., Tao, Z., Chen, L., Ma, X., 2017. The nonlinear oil–water two-phase flow be havior for a horizontal well in triple media carbonate reservoir. Acta Geophys. 65 (5), 977–989.

19.  Wang, Y., Tian, D., Li, G., Zhang, C., Chen, T., 2019. Dynamic analysis of a fractured vertical well in a triple media carbonate reservoir. Chem. Technol. Fuels Oils 55 (1),  56–65.

20.  Wang, Y., Yi, X., 2017. Transient pressure behavior of a fractured vertical well with a finite-conductivity fracture in triple media carbonate reservoir. J. Porous Media 20 (8), 707–722.

## Appendix A. Investigation radius in a homogenous reservoir

The model plan for a well producing at a fixed sandface rate of q in a homogeneous reservoir is shown in Fig.13.1. The radial coordinate is represented by the symbol of r in this image, and the external boundary's radius is represented by re. Using a radial infinitesimal annulus as the shadow area in Fig.13.1, we can calculate the investigation radius calculation formula.

In an infinite reservoir, the pressure wave brought on by well production spreads constantly as production time passes. The reservoir pressure and the radial coordinate in the pressure drop funnel region have a roughly semi-logarithmic relationship in the infinite-acting radial flow state. (Sabet, 1991). The reservoir pressure is stated as follows:

$$p(r,t) = D_1 \ln(r) + D_2, \quad r_{\mathrm{w}} \leq r \leq r_{\mathrm{inv}}(t) \tag{A-1}$$

The wellbore pressure and the wellbore flowing pressure are always equivalent.

$$p(r_{\mathrm{w}}) = p_{\mathrm{wf}}(t) \tag{A-2}$$

The starting reservoir pressure is always equal to the pressure at the front of a pressure drop funnel:

$$p[r_{\mathrm{inv}}(t)] = p_{\mathrm{i}} \tag{A-3}$$

You can determine the reservoir pressure by combining (A-1) and (A-3).

$$p\left(r,t\right) = p_{\mathrm{i}} - \frac{p_{\mathrm{i}} - p_{\mathrm{wf}}(t)}{\ln \frac{r_{\mathrm{inv}}(t)}{r_{\mathrm{w}}}} \ln \frac{r_{\mathrm{inv}}(t)}{r}, \quad r_{\mathrm{w}} \leq r \leq r_{\mathrm{inv}}(t) \tag{A-4}$$

where rw is the wellbore radius, m, rinv(t) is the investigation radius at time t, m, r is the radial radius at any point in the pressure drop funnel area, m, p(r, t) is the reservoir pressure at the radial radius r, Pa$^{-1}$, pwf is the wellbore flowing pressure, Pa, pi is the initial reservoir pressure, Pa$^{-1}$, and D1 and D2 are undetermined coefficients.

According to Marshall (2009) and Guo and Nie (2013), the pressure exponentially affects the porosity and fluid density.

$$\rho = \rho_0 e^{C_L (p - p_0)} \qquad \text{(A-5)}$$

$$\varphi = \varphi_0 e^{C_r (p - p_0)} \qquad \text{(A-6)}$$

where is the fluid density (in kg/m3), is the reservoir porosity (in %), 0, 0, and $p_0$ are any reference values, and $C_L$, $C_r$, and Pa$^{-1}$ are the compressibility's of the fluid and rock, respectively.

Eq. (A-5) times Eq. (A-6) results in

$$\varphi \rho = \varphi_0 \rho_0 e^{(C_r + C_L)(p - p_0)} \qquad \text{(A-7)}$$

You may write the function e using the Maclaurin series expansion by

$$e^x = 1 + x + x^2/2 + \cdots + x^n/n! + \cdots \qquad \text{(A-8)}$$

Eq. (A-7) can be replaced by if we ignore the second and higher order components and utilise the Maclaurin series expansion.

$$\varphi \rho = \varphi_0 \rho_0 \left[ 1 + C_t (p - p_0) \right] \qquad \text{(A-9)}$$

$$C_t = C_L + C_r \qquad \text{(A-10)}$$

where Pa$^{-1}$ equals one and $C_t$ is the total compressibility of rock and fluid.

One may roughly determine the volume of the radial infinitesimal annulus by

$$V_{\inf} = A_{\inf} h = (2\pi r dr) h, \quad r_w \le r \le r_{inv}(t) \qquad \text{(A-11)}$$

where h is the reservoir thickness in m and Vinf is the volume of the infinitesimal annulus, measured in m3. As in is the area of the infinitesimal annulus, measured in m2.

The fluid mass held in the pores of the radial infinitesimal annulus at the initial reservoir conditions can be computed by

$$m_{\inf-i} = V_{\inf} \varphi_i \rho_i = 2\pi r h \varphi_i \rho_i dr, \quad r_w \le r \le r_{inv}(t) \qquad \text{(A-12}$$

where minf-i, in kg, is the starting fluid mass in the infinitesimal annulus under the initial reservoir circumstances; I in percent; and I in kg/m3, is the initial reservoir conditions' porosity and density.

Eq. (A-9) and Eq. (A-12) together allow for a rewriting.

$$m_{\inf-i} = (2\pi r h dr) \varphi_0 \rho_0 \left[ 1 + C_t (p_i - p_0) \right], \quad r_w \le r \le r_{inv}(t) \qquad \text{(A-13)}$$

The fluid mass that is still present in the infinitesimal annulus can be estimated in a similar manner when the production time is t.

$$m_{\text{inf}}(t) = (2\pi r h dr)\varphi_0 \rho_0 \{1 + C_t[p(r,t) - p_0]\}, \quad r_w \leq r \leq r_{\text{inv}}(t) \quad \text{(A-14)}$$

where minf, in kg, is the fluid mass that is still present in the infinitesimal annulus at time t.

The starting fluid mass less the residual fluid mass is essentially the change in fluid mass in the infinitesimal annulus, according to the principle of mass conservation:

$$\Delta m_{\text{inf}} = m_{\text{inf}-i} - m_{\text{inf}}(t) = (2\pi h \varphi_0 \rho_0 C_t)[p_i - p(r,t)]rdr, \quad r_w \leq r \quad \text{(A-15)}$$
$$\leq r_{\text{inv}}(t)$$

where kg represents the change in fluid mass in the smallest annulus, or minf.

As a result, the integral of Eq. (A-15) from the wellbore radius to the investigation radius can be used to determine the total change in fluid mass in the entire pressure-drop funnel area:

$$\Delta m = \int_{r_w}^{r_{\text{inv}}(t)}(\Delta m_{\text{inf}})dr = (2\pi h \varphi_0 \rho_0 C_t)\int_{r_w}^{r_{\text{inv}}(t)}[p_i - p(r,t)]rdr \qquad \text{(A-16)}$$

where kg is the total change in fluid mass along the whole pressure-drop funnel.

Eq. (A-4) into (A-16) substituted results in

$$\Delta m = (\pi h \varphi_0 \rho_0 C_t)\frac{[p_i - p_{wf}(t)]}{\ln\left[\frac{r_{\text{inv}}(t)}{r_w}\right]}\int_{r_w}^{r_{\text{inv}}(t)}2r\ln\left[\frac{r_{\text{inv}}(t)}{r}\right]dr \qquad \text{(A-17)}$$

Parts of the integral term in equation (A-17) can be integrated:

$$\int_{r_w}^{r_{\text{inv}}(t)}2r\ln\left[\frac{r_{\text{inv}}(t)}{r}\right]dr = \left[r^2\ln\frac{r_{\text{inv}}(t)}{r}\right]_{r_w}^{r_{\text{inv}}(t)} \qquad \text{(A-18)}$$
$$- \int_{r_w}^{r_{\text{inv}}(t)}r^2\left[\ln\frac{r_{\text{inv}}(t)}{r}\right]'dr$$

The first term in Equation (A-18right )'s side can be represented as

$$\left[r^2\ln\frac{r_{\text{inv}}(t)}{r}\right]_{r_w}^{r_{\text{inv}}(t)} = -r_w^2\ln\frac{r_{\text{inv}}(t)}{r_w} \qquad \text{(A-19)}$$

The second term in Equation (A-18right )'s side can be represented as

$$- \int_{r_w}^{r_{\text{inv}}(t)}r^2\left[\ln\frac{r_{\text{inv}}(t)}{r}\right]'dr = \int_{r_w}^{r_{\text{inv}}(t)}rdr = \frac{1}{2}r_{\text{inv}}^2(t) - \frac{1}{2}r_w^2 \qquad \text{(A-20)}$$

Equations (A-19) and (A-20) are substituted into Equation (A-18) to produce

$$\int_{r_w}^{r_{\text{inv}}(t)}2r\ln\left[\frac{r_{\text{inv}}(t)}{r}\right]dr = \frac{1}{2}r_{\text{inv}}^2(t) - r_w^2\left[\frac{1}{2} + \ln\frac{r_{\text{inv}}(t)}{r_w}\right] \qquad \text{(A-21)}$$

We determined the values of these two terms by setting "$r_w = 0.1$ m" and a group of investigation radii "$r_{\text{inv}}(t) = 5$ m, 10 m, 50 m, 100 m, 500 m, 1000 m," as indicated in Table A.1 in order to compare the numerical values of the two terms in the right-hand side of Eq. (A-21). All of the values of the first term on the right-hand side of Eq. (A-21) are bigger than 10 $m^2$, while all of the values of the second term are smaller than 0.1 $m^2$, based on the

calculation results presented in Table A.1. For instance, the value of the first term is equal to 12.5 m$^2$ for "$r_{inv}(t) = 5$ m," which is roughly 280 times that of the second term (0.0441 m$^2$).

$$\int_{r_w}^{r_{inv}(t)} 2r \ln\left[\frac{r_{inv}(t)}{r}\right] dr = \frac{1}{2} r_{inv}^2(t) \tag{A-22}$$

Comparisons of the computation results for various inquiry radii are shown in Table A.1.

Table A.1 Comparisons of calculation results for different investigation radiuses

| $r_{inv}(t)$ (m) | $\frac{1}{2} r_{inv}^2(t)$ (m$^2$) | $r_w^2 \left[\frac{1}{2} + \ln\frac{r_{inv}(t)}{r_w}\right]$ (m$^2$) |
|---|---|---|
| 5 | 12.5 | 0.0441 |
| 10 | 50 | 0.0511 |
| 50 | 1250 | 0.0671 |
| 100 | 5000 | 0.0741 |
| 500 | 125000 | 0.0942 |

Substitute Eq. (A-22) into (A-17):

$$\Delta m = \frac{1}{2}(\pi h \varphi_0 \rho_0 C_t) \frac{[p_i - p_{wf}(t)]}{\ln\left[\frac{r_{inv}(t)}{r_w}\right]} r_{inv}^2(t) \tag{A-23}$$

Divide Eq. (A-23) by $\rho_0$:

$$\frac{\Delta m}{\rho_0} = \frac{1}{2}(\pi h \varphi_0 C_t) \frac{[p_i - p_{wf}(t)]}{\ln\left[\frac{r_{inv}(t)}{r_w}\right]} r_{inv}^2(t) \tag{A-24}$$

Since mass is equal to density divided by volume, Eq. (A-24) can be rewritten as

$$\Delta V = \frac{1}{2}(\pi h \varphi_0 C_t) \frac{[p_i - p_{wf}(t)]}{\ln\left[\frac{r_{inv}(t)}{r_w}\right]} r_{inv}^2(t) \tag{A-25}$$

where m represents the entire change in fluid volume throughout the entire pressure-drop funnel area, or V.

The accumulation volume of well production is exactly equal to the total volume change in Eq. (A-25). The accumulation production volume can be determined by using the well production at a constant sand face rate of q and the production time of t.

$$\Delta V = qt \tag{A-26}$$

Equation (A-25) and Equation (A-26) together, the well production rate is stated by

$$q = \frac{1}{2} \frac{(\pi h \varphi_0 C_t)}{t} \frac{[p_i - p_{wf}(t)]}{\ln\left[\frac{r_{inv}(t)}{r_w}\right]} r_{inv}^2(t) \tag{A-27}$$

where q represents the well's m3/s production rate.

The well production rate can be calculated using Darcy's flow by

$$q = A \cdot v = 2\pi r h \cdot \left( \frac{k}{\mu} \frac{dp}{dr} \right) \tag{A-28}$$

where A is the fluid flow's cross-section area in m$^2$, v is the flow's velocity in m/s, k is the reservoir's permeability in m$^2$, and is the fluid's viscosity in Pa/s.

In Eq. (A-28), change the form to:

$$q \frac{1}{r} dr = 2\pi \frac{kh}{\mu} dp \tag{A-29}$$

Integrate Equation (A-29) from the wellbore to the funnel's front:

$$\int_{r_{\mathrm{w}}}^{r_{\mathrm{inv}}(t)} q \frac{1}{r} dr = \int_{p_{\mathrm{wf}}(t)}^{p_i} 2\pi \frac{kh}{\mu} dp \tag{A-30}$$

The integral operation transforms Equation (A-30) into

$$q = \frac{2\pi k h [p_i - p_{\mathrm{wf}}(t)]}{\mu \ \ln\left[ \frac{r_{\mathrm{inv}}(t)}{r_{\mathrm{w}}} \right]} \tag{A-31}$$

Combining equations (A-27) and (A-31) results in

$$r_{\mathrm{inv}}^2 (t) = \frac{4kt}{\varphi_0 \mu C_t} \tag{A-32}$$

As Ø$_0$ is an arbitrary reference value, is typically used in its place. You may rewrite equation (A-32) using

$$r_{\mathrm{inv}} (t) = 2\sqrt{\eta t} = 2\sqrt{\frac{k}{\varphi \mu C_i} t} \tag{A-33}$$

where m$^2$/s is the diffusivity coefficient.

## Appendix B. Investigation radius in a 2-zone composite reservoir

As the pressure wave hits the boundary between the inner and outer zones, we use a radial infinitesimal annulus in the outer zone (the second zone), as shown in Fig. B.1, to calculate the calculation formula for the investigation radius.
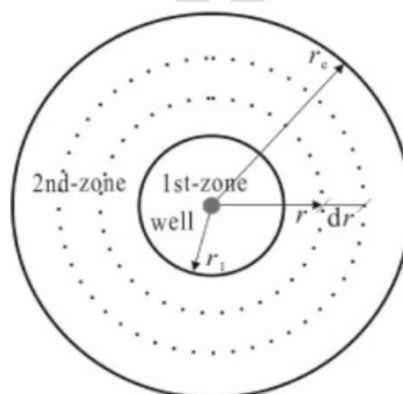


Fig-B.1  Model scheme of composite reservoir

The reservoir pressure and the radial coordinate have an approximately semi-logarithmic connection when the 2-zone composite reservoir has an infinite boundary and an infinite-acting radial flow state (Sabet, 1991). The second-zone reservoir pressure can be expressed as

$$p_2(r,t) = C_1 \ln(r) + C_2, \quad r_1 \le r \le r_{\text{inv}}(t) \tag{B-1}$$

At the boundary between the inner zone and the outer zone, the reservoir pressure is

$$p_2(r_1) = p_{r1}(t) \tag{B-2}$$

The reservoir pressure in the second zone can be obtained by combining (B-1) and (B-3).

$$p_2[r_{\text{inv}}(t)] = p_i \tag{B-3}$$

By combining (B-1) and (B-3), it is possible to determine the reservoir pressure in the second zone.

$$p_2\left(r,t\right) = p_i - \frac{p_i - p_{r1}(t)}{\ln \frac{r_{\text{inv}}(t)}{r_1}} \ln \frac{r_{\text{inv}}(t)}{r}, \quad r_1 \le r \le r_{\text{inv}}(t) \tag{B-4}$$

where $p_2(r, t)$ is the reservoir pressure of the second zone at the radial radius of $r_o$, Pa; $p_{r1}$ is the reservoir pressure at the radial radius of $r_1$, Pa; $p_i$ is the initial reservoir pressure, Pa; $C_1$ and $C_2$ are undetermined coefficients. $r_{\text{inv}}(t)$ is the investigation radius at time t, in m.

When fluid density and porosity are influenced by pressure in an exponential manner (Marshall, 2009; Guo and Nie, 2013):

$$\rho_2 = \rho_0 e^{C_{L2}(p_2 - p_0)} \tag{B-5}$$

$$\varphi_2 = \varphi_0 e^{C_{r2}(p_2 - p_0)} \tag{B-6}$$

where $\rho_2$ is the second-zone liquid density in kg/m$^3$; $\varphi_2$ is the second-zone porosity in percentage; $\rho_0$, $\varphi_0$, and $p_0$ are any reference values; $C_{L2}$ is the second-zone fluid compressibility; and $C_{r2}$ is the second-zone rock compressibility.

Eq. (B-5) becomes Eq. (B-6) when multiplied by it.

$$\varphi_2 \rho_2 = \varphi_0 \rho_0 e^{(C_{r2} + C_{L2})(p_2 - p_0)} \tag{B-7}$$

Eq. (B-7) can be replaced by if the Maclaurin series expansion is applied, ignoring the second and higher order elements (see Eq. (A-8) in Appendix A).

$$\varphi_2 \rho_2 = \varphi_0 \rho_0 [1 + C_{t2}(p_2 - p_0)] \tag{B-8}$$

$$C_{t2} = C_{L2} + C_{r2} \tag{B-9}$$

where Pa$^{-1}$ is the first-zone pressure, and $C_{t2}$ is the total compressibility.

One may roughly determine the volume of the radial infinitesimal annulus by

$$V_{\text{inf}} = A_{\text{inf}} h = (2\pi r dr) h, \quad r_1 \le r \le r_{\text{inv}}(t) \tag{B-10}$$

where h is the reservoir thickness in m and Vinf is the volume of the infinitesimal annulus, measured in $m^3$. A $r_{inv}$ is the area of the infinitesimal annulus, measured in $m^2$.

The fluid mass held in the pores of the radial infinitesimal annulus at the initial reservoir conditions can be computed by

$$m_{\text{inf}-i} = V_{\text{inf}}\varphi_{2i}\rho_{2i} = 2\pi rh\varphi_{2i}\rho_{2i}dr, \quad r_1 \leq r \leq r_{\text{inv}}(t) \tag{B-11}$$

where I is the initial porosity in the initial reservoir circumstances, percent; I is the initial reservoir conditions density, kg/m3; and $m_{\text{inf-i}}$ is the initial fluid mass in the infinitesimal annulus in the initial reservoir conditions, kg.

Combining Eq. (B-8) and Eq. (B-11), one can rewrite

$$m_{\text{inf}-i} = (2\pi rhdr)\,\varphi_0\rho_0\left[1 + C_{t2}\left(p_i - p_0\right)\right], \quad r_1 \leq r \leq r_{\text{inv}}(t) \tag{B-12}$$

The fluid mass that is still present in the infinitesimal annulus can be estimated in a similar manner when the production time is t.

$$m_{\text{inf}}(t) = (2\pi rhdr)\,\varphi_0\rho_0\left\{1 + C_{t2}\left[p_2(r,t) - p_0\right]\right\}, \quad r_1 \leq r \tag{B-13}$$
$$\leq r_{\text{inv}}(t)$$

where $m_{\text{inf}}$, in kg, is the fluid mass that is still present in the infinitesimal annulus at time t.

The starting fluid mass less the residual fluid mass is essentially the change in fluid mass in the infinitesimal annulus, according to the principle of mass conservation:

$$\Delta m_{\text{inf}} = m_{\text{inf}-i} - m_{\text{inf}}(t) = (2\pi h\varphi_0\rho_0 C_{t2})\left[p_i - p_2(r,t)\right]rdr, \quad r_1 \tag{B-14}$$
$$\leq r \leq r_{\text{inv}}(t)$$

where kg represents the change in fluid mass in the smallest annulus, or $m_{\text{inf}}$.

As a result, the integral of Eq. (B-14) from the radius of the first zone to the investigation radius can be used to determine the total change in fluid mass throughout the entire pressure-drop area in the second zone.

$$\Delta m = \int_{r_1}^{r_{\text{inv}}(t)} (\Delta m_{\text{inf}})dr = (2\pi h\varphi_0\rho_0 C_{t2})\int_{r_1}^{r_{\text{inv}}(t)}\left[p_i - p_2(r,t)\right]rdr \tag{B-15}$$

where kg represents the overall change in fluid mass throughout the whole pressure-drop region of the second zone.

Replace Equation (B-4) in Equation (B-15):

$$\Delta m = (\pi h\varphi_0\rho_0 C_{t2})\frac{\left[p_i - p_{r1}(t)\right]}{\ln\left[\frac{r_{\text{inv}}(t)}{r_1}\right]}\int_{r_1}^{r_{\text{inv}}(t)} 2r\,\ln\left[\frac{r_{\text{inv}}(t)}{r}\right]dr \tag{B-16}$$

Parts of the integral term in equation (B-16) can be integrated:

$$\int_{r_1}^{r_{inv}(t)} 2r \, \ln\left[\frac{r_{inv}(t)}{r}\right] dr = \left[r^2 \, \ln\frac{r_{inv}(t)}{r}\right]_{r_1}^{r_{inv}(t)} - \int_{r_1}^{r_{inv}(t)} r^2 \left[\ln\frac{r_{inv}(t)}{r}\right]' dr \tag{B-17}$$

The first term in Equation (B-17right's ) side can be represented as

$$\left[r^2 \, \ln\frac{r_{inv}(t)}{r}\right]_{r_1}^{r_{inv}(t)} = -r_1^2 \, \ln\frac{r_{inv}(t)}{r_1} \tag{B-18}$$

The second term in the equation (B-17right's ) side can be represented as follows.

$$-\int_{r_1}^{r_{inv}(t)} r^2 \left[\ln\frac{r_{inv}(t)}{r}\right]' dr = \int_{r_1}^{r_{inv}(t)} r\,dr = \tfrac{1}{2}r_{inv}^2(t) - \tfrac{1}{2}r_1^2 \tag{B-19}$$

Eq. (B-17) is replaced by Eqs. (B-18) and (B-19) as follows:

$$\int_{r_1}^{r_{inv}(t)} 2r \, \ln\left[\frac{r_{inv}(t)}{r}\right] dr = \tfrac{1}{2}r_{inv}^2(t) - r_1^2\left[\tfrac{1}{2} + \ln\frac{r_{inv}(t)}{r_1}\right] \tag{B-20}$$

$$\int_{r_1}^{r_{inv}(t)} 2r \, \ln\left[\frac{r_{inv}(t)}{r}\right] dr = \tfrac{1}{2}r_{inv}^2(t) - r_1^2\left[\tfrac{1}{2} + \ln\frac{r_{inv}(t)}{r_1}\right] \tag{B-20}$$

As indicated in Table B.1, we calculated the values of the two terms by setting "$r_1$ = 100 m" and a group of investigation radii " $r_{inv}(t)$ = 150 m, 200 m, 300 m, 500 m, 1000 m" in order to examine the numerical differences between the two terms in the right-hand side of Eq. (B-20). The value of the first term at " $r_{inv}(t)$ = 150 m" is equal to 11250 m², which is less than the value of the second term (18109 m²), per the calculation results displayed in Table B.1. The first term's value is only 2.96 times that of the second term (42188 m²) at "$r_{inv}(t)$ = 500 m," or 125000 m². In light of this, when contrasted to the first term in the right side of Eq.

TableB.1. Comparisons of calculation results for different investigation radii

| $r_{inv}(t)$ **(m)** | $\tfrac{1}{2}r_{inv}^2(t)$ **(m²)** | $r_1^2\left[\tfrac{1}{2} + \ln\frac{r_{inv}(t)}{r_1}\right]$ **(m²)** |
|---|---|---|
| 150 | 11250 | 18109 |
| 200 | 20000 | 23862 |
| 300 | 45000 | 31972 |
| 500 | 125000 | 42188 |
| 1000 | 500000 | 56051 |

Eq. (B-20) should be used in place of Eq.

$$\Delta m = (\pi h \varphi_0 \rho_0 C_{t2}) \frac{[p_i - p_{r1}(t)]}{\ln\left[\frac{r_{inv}(t)}{r_1}\right]} \left\{ \frac{1}{2} r_{inv}^2(t) - r_1^2 \left[\frac{1}{2} + \ln \frac{r_{inv}(t)}{r_1}\right]\right\} \qquad \text{(B-21)}$$

Divide Eq. (B-21) by $\rho_0$:

$$\frac{\Delta m}{\rho_0} = (\pi h \varphi_0 C_{t2}) \frac{[p_i - p_{r1}(t)]}{\ln\left[\frac{r_{inv}(t)}{r_1}\right]} \left\{ \frac{1}{2} r_{inv}^2(t) - r_1^2 \left[\frac{1}{2} + \ln \frac{r_{inv}(t)}{r_1}\right]\right\} \qquad \text{(B-22)}$$

As mass is equal to density divided by volume, Eq. (B-22) can be rewritten as

$$\Delta V = (\pi h \varphi_0 C_{t2}) \frac{[p_i - p_{r1}(t)]}{\ln\left[\frac{r_{inv}(t)}{r_1}\right]} \left\{ \frac{1}{2} r_{inv}^2(t) - r_1^2 \left[\frac{1}{2} + \ln \frac{r_{inv}(t)}{r_1}\right]\right\} \qquad \text{(B-23)}$$

where m$^3$ represents the overall change in fluid volume along the whole pressure-drop funnel area of the second zone, V.

The time at which the pressure wave hits the boundary between the inner and outer zones can be determined using Eq.

$$t_1 = \frac{r_1^2}{4\eta_1} = \frac{\varphi_1 \mu_1 C_{t1} r_1^2}{4k_1} \qquad \text{(B-24)}$$

where $t_1$ is the time, in seconds, at which the pressure wave reaches the first-zone-to-second-zone interface; $\eta_1$ is the first-diffusivity zone's coefficient, measured in m$^2$/s; $k_1$ is its permeability, measured in m$^2$; $\varphi_1$ is its porosity, measured in fraction; $\mu_1$ is its fluid viscosity, measured in Pa/s; and $C_{t1}$ is its overall compressibility, measured in Pa/s.

The accumulation fluid volume out of the second zone is exactly equal to the overall change in fluid volume across the entire pressure-drop funnel region of the second zone. The flow rate at the boundary between the first zone and the second zone is equal to q as a result of well production at a constant sand face rate of q. The buildup by the production time t

$$\Delta V = q(t - t_1) \qquad \text{(B-25)}$$

The flow rate at the boundary between the first zone and the second zone can be expressed by combining equations (B-24) and (B-25).

$$q = \frac{1}{2} \frac{(\pi h \varphi_0 C_{t2})}{t - t_1} \frac{[p_i - p_{r1}(t)]}{\ln\left[\frac{r_{inv}(t)}{r_1}\right]} \left\{ \frac{1}{2} r_{inv}^2(t) - r_1^2 \left[\frac{1}{2} + \ln \frac{r_{inv}(t)}{r_1}\right]\right\} \qquad \text{(B-26)}$$

Considering Darcy's flow, the flow rate at the radius of $r$ can be calculated by

$$q = A \cdot v = 2\pi r h \cdot \left(\frac{k_2}{\mu_2} \frac{dp}{dr}\right), \quad r_1 \le r \le r_{inv}(t) \qquad \text{(B-27)}$$

where A is the fluid flow cross-section area in m$^2$, v is the fluid flow speed in m/s, $k_2$ is the fluid permeability in m$^2$ of the second zone, and $\mu_2$ is the fluid viscosity in s of the second zone.

In Eq. (B-27), change the form to:

$$q\frac{1}{r}dr = 2\pi\frac{k_2 h}{\mu_2}dp, \quad r_1 \le r \le r_{inv}(t) \tag{B-28}$$

Integrate Equation (B-28) from the first-zone to second-zone interface to the pressure drop funnel's front:

$$\int_{r_1}^{r_{inv}(t)} q\frac{1}{r}dr = \int_{p_{r1}(t)}^{p_i} 2\pi\frac{kh}{\mu}dp \tag{B-29}$$

The integral operation transforms Equation (B-29) into

$$q = \frac{2\pi k_2 h[p_i - p_{r1}(t)]}{\mu_2 \ln\left[\frac{r_{inv}(t)}{r_1}\right]} \tag{B-30}$$

Equation (B-26) and Equation (B-30) together yield

$$r_{inv}^2(t) - 2r_1^2 \ln r_{inv}(t) - r_1^2 + 2r_1^2 \ln r_1 = \frac{4k_2}{(\varphi_0 \mu_2 C_{t2})}(t - t_1) \tag{B-31}$$

Because $\varphi_0$ is an arbitrary reference value, it is usually replaced by $\varphi_2$. Eq(B-31) can be rewritten by

$$r_{inv}^2(t) - 2r_1^2 \ln r_{inv}(t) - r_1^2 + 2r_1^2 \ln r_1 = \frac{4k_2}{\varphi_2 \mu_2 C_{t2}}(t - t_1) \tag{B-32}$$

$$r_{inv}^2(t) - 2r_1^2 \ln r_{inv}(t) - r_1^2 + 2r_1^2 \ln r_1 = 4\eta_2(t - t_1) \tag{B-33}$$

where 2 is the diffusivity coefficient, m2/s; k2 is the permeability of the second zone, m2; $\varphi_2$ is the second zone's porosity, percent; 2 is the second zone's fluid viscosity, Pa-s; and $C_{t2}$ is the second zone's total compressibility, Pa1.

The investigation radius for a single well production in a 2-zone composite reservoir can be determined using Equations (B-32) and (B-33).s